

CLUSTERED FLEXIBLE CALIBRATION PLOTS FOR BINARY OUTCOMES USING RANDOM EFFECTS MODELING

Lasai Barreñada^{1,2}, Bavo D.C. Campo^{1,3,4}, Laure Wynants^{1,2,5}, Ben Van Calster^{1,2}

¹ Department of Development and Regeneration, KU Leuven, Belgium

² Leuven Unit for Health Technology Assessment Research (LUHTAR), KU Leuven, Belgium

³ Department of Metabolism, Digestion and Reproduction, Imperial College, United Kingdom.

⁴ Department of Accountancy, Finance and Insurance, KU Leuven, Belgium

⁵ Department of Epidemiology, CAPHRI Care and Public Health Research Institute, Maastricht University, Maastricht, Netherlands.

Corresponding author

Ben Van Calster

KU Leuven, Department of Development and Regeneration

Herestraat 49 box 805

3000 Leuven

Belgium

Ben.vancalster@kuleuven.be

Evaluation of clinical prediction models across multiple clusters, whether centers or datasets, is becoming increasingly common. A comprehensive evaluation includes an assessment of the agreement between the estimated risks and the observed outcomes, also known as calibration. Calibration is of utmost importance for clinical decision making with prediction models and it may vary between clusters. We present three approaches to take clustering into account when evaluating calibration. (1) Clustered group calibration (CG-C), (2) two stage meta-analysis calibration (2MA-C) and (3) mixed model calibration (MIX-C) can obtain flexible calibration plots with random effects modelling and providing confidence and prediction intervals. As a case example, we externally validate a model to estimate the risk that an ovarian tumor is malignant in multiple centers ($N = 2489$). We also conduct a simulation study and synthetic data study generated from a true clustered dataset to evaluate the methods. In the simulation and the synthetic data analysis MIX-C gave estimated curves closest to the true overall and center specific curves. Prediction interval was best for 2MA-C with splines. Standard flexible calibration worked likewise in terms of calibration error when sample size is limited. We recommend using 2MA-C (splines) to estimate the curve with the average effect and the 95% PI and MIX-C for the cluster specific curves, specially when sample size per cluster is limited. We provide ready-to-use code to construct summary flexible calibration curves with confidence and prediction intervals to assess heterogeneity in calibration across datasets or centers.

Highlights

What is already known

Traditional methods for assessing calibration in clinical prediction models often assume independence between observations. However, when performing an external validation where the data is clustered, this assumption is violated. Ignoring clustering can impair the reliability of calibration assessments, potentially leading to misguided clinical decisions.

What is new

We introduce three novel methodologies that explicitly account for clustering in calibration assessments during clinical prediction model validation. These methods generate an overall calibration curve with prediction intervals, representing expected calibration curves in hypothetical new centers. Among these, the MIX-C method is particularly recommended, as it provides center-specific calibration curves and prediction intervals. To facilitate adoption, we provide ready-to-use R functions.

Potential impact for Research Synthesis Methods readers

External validations aim to assess how clinical prediction models perform across diverse external settings. Neglecting the clustered nature of data in multicenter validations or meta-analyses of validation studies undermines calibration analysis, overlooking center-specific insights. The methodologies we propose address these limitations by estimating summary calibration curves and offering prediction intervals for hypothetical new centers. This approach enables more refined and reliable calibration assessments, directly supporting informed decision-making in clinical research.

1 INTRODUCTION

Clinical prediction models (CPMs) are evidence based tools that estimate the probability of health-related events either at the time of evaluation (diagnosis) or at some point in the future (prognosis).^{1,2} These risk estimates play a crucial role in evidence-based decision-making and can be of great value when counseling patients. However, to ensure the reliability of risk estimates, CPMs must exhibit good calibration.³ Calibration assesses how well the predicted risks corresponded to observed risks.⁴ In recent years, there has been a notable increase in studies involving multiple clusters. The term "cluster" can refer to different groupings within the population under study, depending on the context. For example, in multicenter studies, a cluster commonly refers to different centers, whereas in meta-analysis, a cluster may pertain to each study or centers within the study where possible (e.g. individual patient data (IPD) meta-analysis⁵). In this work, the term "cluster" will specifically denote a center in a multicenter study, but the methods proposed apply more generally as well. An analysis of CPMs included in Tufts PACE (Predictive Analytics + Comparative Effectiveness), developed after the year 2000, revealed that 64% of the models utilized multicenter (clustered) data, indicating a growing trend in such studies.^{6,7} TRIPOD (Transparent Reporting of a Multivariable Prediction Model for Individual Prognosis or Diagnosis) has addressed this development by publishing an extension known as TRIPOD-Cluster.⁸ This extension underscores the importance of taking clustering into account when developing or evaluating prediction models.

Miscalibration can have a harmful influence on medical decision making.³ It is common to observe heterogeneity in model performance across centers or studies, most notably in model calibration.^{9–12} It can thus be misleading to generalize performance results from single-cluster data.^{13–16} For these reasons, it is crucial to collect clustered data to investigate and quantify heterogeneity in calibration performance between clusters. The presence of clustering introduces challenges, as individuals are no longer independent due to correlations among patients within the same cluster.^{17,18} Traditional (non-clustered) methodologies should therefore be adapted for use with clustered data.

The most informative assessment of calibration performance for a prediction model is a calibration plot, to assess whether, among patients with the same estimated risk of the event, the observed proportion of events equals the estimated risk.^{4,19} Summarizing calibration statistics exist, such as the observed over expected (O:E) ratio, calibration intercept, calibration slope, expected calibration error (ECE), estimated calibration index (ECI) or integrated calibration index (ICI). Such summarizing statistics are by definition less informative than the calibration plot.¹⁹

A calibration plot has estimated risks on the x-axis, and the observed proportion on the y-axis. For binary outcomes, observed outcome values are $Y = 0$ (no event) or $Y = 1$ (event). The observed proportion of individuals with the event conditional on estimated risk are not observed directly, but are estimated. One approach consists of creating Q groups (usually based on quantiles of estimated risks) and estimating the observed proportion in each of the groups as the proportion of individuals with the condition. We refer to this approach throughout the text as grouped calibration. The calibration plot then has Q dots representing the mean risk (value on the x-axis) and observed proportion (value on the y-axis). Another approach is using a flexible model.²⁰ The observed outcome is regressed on the estimated probabilities using a smoother such as local regression (loess) or splines. The smoothed relation or Q groups are plotted together with a line of identity which represents perfect calibration. The grouped approach loses information by categorizing the estimated risks, and depends on the value of Q and the grouping approach. Flexible models are dependent on smoothing parameters. Flexible calibration curves have been presented for different problems like survival models²¹, competing risk models²² or multiclass models²³. However, we did not find work that presents flexible calibration curves that are able to

consider clustering. We present three different approaches to construct flexible calibration curves from clustered data, provide center-specific curves, and quantify heterogeneity using prediction intervals. We present results for a real case example, simulated data, and synthetic data. This study is an initial assessment of methods for clustered calibration analysis that we classify as a phase 2 methodological study in the four phase framework from Heinze and colleagues.²⁴

2 METHODS

2.1 MOTIVATING EXAMPLE: ADNEX MODEL AND OVARIAN CANCER DATA

The methods will be illustrated using the ADNEX model for ovarian tumor discrimination that was developed with data from the International Ovarian Tumor Analysis (IOTA) group.^{25,26} The ADNEX model is a multinomial regression mixed model with random intercepts per center to estimate the probability that an ovarian mass is malignant. Predicting malignancy of ovarian masses prior to surgery is important because benign masses can be managed conservatively, and malignant masses require different surgical approaches depending on the malignant subtype. ADNEX estimates the risk of five outcomes: benign tumor, borderline tumor, stage I invasive cancer, stage II-IV invasive cancer, and secondary metastasis. This work will focus on the overall risk of malignancy, which is obtained by adding the risks for the malignant subtypes. ADNEX has three clinical and six ultrasound predictors: age, serum CA125 level, type of center (oncology center or other hospital type), maximal diameter of the lesion, proportion of solid tissue, number of papillary projections, presence of >10 locules, acoustic shadows, and ascites. CA125 is optional, and in this work we focus on ADNEX without CA125. ADNEX coefficients already capture some of the between center heterogeneity through the type of center. To illustrate multicenter calibration of the ADNEX model we use an external validation dataset of 2489 patients recruited in 17 hospitals.²⁷ Previous external validation of ADNEX on this dataset suggested that there was important heterogeneity between hospitals (**Figure S1**).⁹ To avoid computation errors, three small non-oncology centers in Italy were combined, as well as two small non-oncology centers in the United Kingdom. The dataset then contains 14 clusters, with a median number of 189 patients per cluster (range 38 to 360) (**Figure 1**). The mean estimated probabilities (range 0.10 to 0.53) and the prevalence of malignancy (range 0.16 to 0.72) varied between clusters. The intra cluster correlation (ICC) in (logit) malignancy risk based on the null random intercept model is 15%.¹⁷ An ICC of 0 would mean that all centers are similar, and all variance in the logit malignancy risk is due to individual-level variability.

2.2 NOTATION

We assume to have a dataset with a total of J clusters and use $j = (1, \dots, J)$ to index the clusters. In each cluster, we have n_j patients and we index the patients using $i = (1, \dots, n_j)$. The total sample size is $N = \sum_{j=1}^J n_j$. We use $y_{ij} \in (0,1)$ to denote the outcome of patient i in cluster j , which takes on the value 0 in case of a non-event and 1 in case of an event. We assume that y_{ij} follows a Bernoulli distribution $y_{ij} \sim \text{Bern}(\pi_{ij})$, where π_{ij} denotes the probability of experiencing the event. Typically, π_{ij} is expressed as a function of a set of risk characteristics, captured in the covariate vector \mathbf{x}_{ij} and we assume that there exists an unknown regression function $r(\mathbf{x}_{ij}) = P(y_{ij} = 1 | \mathbf{x}_{ij})$. We approximate this function using a risk prediction model, where we model the outcome as a function of the observed risk characteristics and employ statistical or machine learning techniques to estimate this model. A general expression that encompasses both types is

$$P(y_{ij} = 1 | \mathbf{x}_{ij}) = \pi(\mathbf{x}_{ij}) = f(\mathbf{x}_{ij}) \quad (1)$$

In a logistic regression model, we have that

$$\pi(\mathbf{x}_{ij}) = \frac{e^{\mathbf{x}_{ij}^T \boldsymbol{\beta}}}{1 + e^{\mathbf{x}_{ij}^T \boldsymbol{\beta}}}$$

where $\boldsymbol{\beta}$ denotes the parameter vector. We use $\eta_{ij} = \mathbf{x}_{ij}^T \boldsymbol{\beta}$ to represent the linear predictor. We can rewrite the above equation to

$$\begin{aligned} \log\left(\frac{\pi(\mathbf{x}_{ij})}{1 - \pi(\mathbf{x}_{ij})}\right) &= \mathbf{x}_{ij}^T \boldsymbol{\beta} \\ \text{logit}\left(\pi(\mathbf{x}_{ij})\right) &= \mathbf{x}_{ij}^T \boldsymbol{\beta} \end{aligned}$$

We can employ splines to allow for a non-linear relationship between the covariates and outcome. To estimate equation (1), we fit a statistical or machine learning model to the training data. The resulting model fit then provides us with the predicted probability $\hat{\pi}(\mathbf{x}_{ij}) = \hat{f}(\mathbf{x}_{ij})$.

Using calibration curves, we examine how well the predicted probabilities correspond to the actual event probabilities^{1,4,28,29}. A calibration plot maps the predicted probabilities $\hat{\pi}(\mathbf{x}_{ij})$ to the actual event probabilities $P(y_{ij} = 1 \mid \hat{\pi}(\mathbf{x}_{ij}))$ and hereby provides a visual representation of the alignment between the model's estimated risks and the true probabilities. For a perfectly calibrated model, the calibration curve follows the diagonal as $P(y_{ij} = 1 \mid \hat{\pi}(\mathbf{x}_{ij})) = \pi(\mathbf{x}_{ij}) \forall i$ where $\forall i$ denotes for all i .

2.3 FLEXIBLE CALIBRATION PLOTS IGNORING CLUSTERING

We can estimate the calibration curve using a logistic regression model²⁹⁻³¹

$$\text{logit}\left(P(y_{ij} = 1 \mid \hat{\pi}(\mathbf{x}_{ij}))\right) = \alpha + \zeta \text{logit}\left(\hat{\pi}(\mathbf{x}_{ij})\right)$$

where we estimate the observed proportions as a function of the (logit transformed) predicted probabilities. Using the fitted model, we create a calibration curve by plotting the $\hat{\pi}(\mathbf{x}_{ij})$ against the observed proportions $\hat{P}(y_{ij} = 1 \mid \hat{\pi}(\mathbf{x}_{ij}))$. This model, however, only allows for a linear relationship and, as such, does not adequately capture moderate calibration. To allow for a non-linear relationship between $\hat{\pi}(\mathbf{x}_{ij})$ and y_{ij} , we can rely on non-parametric smoothers, such as locally estimated scatterplot smoothing (loess) or restricted cubic splines

$$\text{logit}\left(P(y_{ij} = 1 \mid \hat{\pi}(\mathbf{x}_{ij}))\right) = s\left(\text{logit}\left(\hat{\pi}(\mathbf{x}_{ij})\right)\right).$$

Here, $s(\cdot)$ denotes the smooth function applied to the logit transformed predicted probability. This results in a flexible calibration plot, which is implemented in R packages such as `CalibrationCurves` (`val.prob.ci.2` function), `rms` (`val.prob.ci` function), or `tidyverse` (`cal_plot_logistic` function).^{4(p20),32,33}

Figure 2 presents a flexible calibration curve (using a restricted cubic spline) based on the motivating example with pooled data, and the results of a grouped calibration assessment for ovarian malignancy prediction. The panel below shows the sample distribution of the estimated risks for benign cases (blue) and malignant cases (red). The plots suggest that risks were estimated too low.

Since there is no commonly accepted way to estimate calibration curves for prediction models in clustered data, we present three approaches covering different statistical methodologies. First, we present a grouped clustered calibration plot based on a bivariate random effects meta-analysis model (Clustered Group Calibration; CG-C). Second, we introduce a two stage univariate random effects meta-

analytical approach for the estimation of the observed events (Two stage meta-analysis calibration; 2MA-C). Finally, we provide a one-step approach where we fit a random effects model with smooth effects to obtain individual calibration slopes per center (Mixed model calibration; MIX-C). We present the summary of the three proposed approaches in **Table 1**.

2.4 CLUSTERED GROUP CALIBRATION (CG-C)

CG-C approach is a two-stage approach that extends the traditional grouped calibration approach to clustered data. In the traditional approach, data is pooled and groups are created based on quantiles (often deciles). In CG-C, we create Q quantiles in every cluster (based on the estimated risk distribution per cluster) with $q = (1, \dots, Q)$. Hereafter, we pool the estimated risks and observed proportions with bivariate random effects meta-analysis where the random factor is the cluster and the response variables the logit-transformed observed proportion and average estimated risk. The equation of this model is given by

$$\begin{bmatrix} \text{logit}(\bar{y}_{qj}) \\ \text{logit}(\bar{\pi}_{qj}) \end{bmatrix} = \begin{bmatrix} \bar{y}\mu_q + u_{qj} + \varepsilon_{qj} \\ \bar{\pi}\mu_q + v_{qj} + \epsilon_{qj} \end{bmatrix} \quad (2)$$

where \bar{y}_{qj} denotes the observed proportion in quantile q and $\bar{\pi}_{qj}$ the average estimated risk in quantile q . We use the subscript q in the quantities to indicate that this refers to quantile q . u_{qj} and v_{qj} represent the random intercepts for cluster j , capturing the between-cluster heterogeneity whereas ε_{qj} and ϵ_{qj} account for the within-cluster error. In this model, we assume that $\bar{y}\mu_q + u_{qj}$ and $\bar{\pi}\mu_q + v_{qj}$ are randomly drawn from a distribution with mean (or pooled) $\bar{y}\mu_q$ and $\bar{\pi}\mu_q$, respectively. Additionally, we assume that

$$\begin{bmatrix} u_{qj} \\ v_{qj} \end{bmatrix} \sim \mathcal{N} \left(\begin{bmatrix} 0 \\ 0 \end{bmatrix}, \Omega \right) \text{ and } \begin{bmatrix} \varepsilon_{qj} \\ \epsilon_{qj} \end{bmatrix} \sim \mathcal{N} \left(\begin{bmatrix} 0 \\ 0 \end{bmatrix}, \Sigma_q \right)$$

where Ω and Σ_q represent the between-cluster and within-cluster covariance matrices, respectively.

$$\Omega = \begin{bmatrix} q\tau_{\bar{y}}^2 & b\rho_q & q\tau_{\bar{y}}^2 & q\tau_{\bar{\pi}}^2 \\ b\rho_q & q\tau_{\bar{y}}^2 & q\tau_{\bar{\pi}}^2 & q\tau_{\bar{\pi}}^2 \end{bmatrix}$$

$$\Sigma_q = \begin{bmatrix} \bar{y}\sigma_{qj}^2 & w\rho_q & \bar{y}\sigma_{qj}^2 & \bar{\pi}\sigma_{qj} \\ w\rho_q & \bar{y}\sigma_{qj}^2 & \bar{\pi}\sigma_{qj}^2 & \bar{\pi}\sigma_{qj} \end{bmatrix}$$

We use $\bar{y}\sigma_{qj}^2$ and $\bar{\pi}\sigma_{qj}^2$ to denote the variance of \bar{y}_{qj} and $\bar{\pi}_{qj}$, $w\rho_q$ represents the within-cluster correlation and $b\rho_q$ the between-cluster correlation. The between-study variance is denoted as $q\tau_{\bar{y}}^2$ and $q\tau_{\bar{\pi}}^2$. We use a bivariate meta-analysis model to account for the strong correlation between the average estimated risk and observed proportion. This approach has the advantage of obtaining an observed proportion per cluster in a model agnostic way and providing uncertainty measures in the cluster with average random effect with confidence intervals for that effect and in a hypothetical new cluster (PI; prediction intervals). It also has some limitations. First, it has the same drawback as the traditional grouped calibration because the curve is dependent on the number of quantiles selected, especially when the sample size is limited. Second, and linked to previous limitation, the arbitrary selection of Q quantiles might create groups that are too heterogeneous between clusters because the estimated risks distributions differ (e.g. a high risk setting vs a low risks setting). Third, the meta-analysis does not provide cluster-specific curves using empirical Bayes. We used the `rma.mv` function of the `metafor` package.³⁴

We include an extension to the proposed methodology that we call “interval” grouping. The methodology is the same except for the way the groups are created. Per cluster, we create I groups by dividing the probability space (0-1) in I equally spaced intervals. In this way we will create I groups of different sizes based on the estimated risks. By doing this we reduce the within group variability at the expense of not having necessarily all clusters present in all I groups. The algorithm and illustrations are available in **Supporting material (Appendix A1, Figure S2-S5) and code for the implementation in OSF repository** (<https://osf.io/aj8ew/>)³⁵.

2.5 TWO STAGE META-ANALYSIS CALIBRATION (2MA-C)

For the second approach we use a two stage random effects meta-analysis to estimate the calibration plot. First, we fit a flexible curve per center with a smoother of choice. Currently, we implemented restricted cubic splines and LOESS. For LOESS, in each center, the span parameter with lowest bias-corrected AIC is selected. For restricted cubic splines the number of knots per center is selected by performing a likelihood ratio test between all combinations of models with 3,4 and 5 knots selecting the model with the least knots that provides the best fit. We train a flexible curve per center and estimate the observed proportion for a fixed grid of estimated risks from 0.01 to 0.99 (default is 100 points). Hereafter, we use a random effects meta-analysis model per point in the grid to combine the logit transformed predictions across centers, fitting the following univariate model per point i in the grid

$$\text{logit}({}_s\hat{\pi}_{ij}) = \hat{\pi}\mu_i + v_{ij} + \epsilon_{ij}.$$

${}_s\hat{\pi}_{ij}$ denotes the predicted proportion of point i for center j , $\hat{\pi}\mu_i$ the overall mean for point i , v_{ij} the center-specific deviation and ϵ_{ij} the error. We assume that $v_{ij} \sim \mathcal{N}(0, {}_i\tau_{\hat{\pi}}^2)$ and $\epsilon_{ij} \sim \mathcal{N}(0, \hat{\pi}\sigma_{ij}^2)$. Further, we include the inverse of the variance of $\text{logit}({}_s\hat{\pi}_{ij})$ as weight and hereby take both the center-specific ($\hat{\pi}\sigma_{ij}^2$) and between-center variability (${}_i\tau_{\hat{\pi}}^2$) into account. As such, clusters with a more precise estimates are assigned greater weights. This approach has the strength of being easy to compute and providing heterogeneity measures for the cluster with average calibration. This allows to plot confidence and prediction intervals which help to visually assess the certainty of the average curve (CI) and the heterogeneity between hypothetical new centers (PI) in the whole range of predicted probabilities. The main limitation is that it is based on the smoothing technique used in each individual cluster so the curves will vary depending on the smoother selected. Additionally, the technique treats each point in the grid as independent, leading to pointwise confidence and prediction intervals. Cluster specific curves are obtained in the first stage independently from the rest of clusters. The algorithm and illustration are available in **Supporting material (Appendix A2, Figure S6-S7) and code for the implementation in OSF repository** (<https://osf.io/aj8ew/>)

2.6 MIXED MODEL CALIBRATION (MIX-C)

In the third approach, we employ a one-stage logistic generalized linear mixed model (GLMM) to model the outcome as a function of the logit transformed predictions. To allow for a non-linear effect, we employ restricted cubic splines with three knots for both the fixed and random effects

$$\text{logit}\left(\text{P}(y_{ij} = 1 \mid \hat{\pi}(\mathbf{x}_{ij}), \tilde{s}_j)\right) = s\left(\text{logit}\left(\hat{\pi}(\mathbf{x}_{ij})\right)\right) + \tilde{s}_j\left(\text{logit}\left(\hat{\pi}(\mathbf{x}_{ij})\right)\right).$$

Here, \tilde{s}_j denotes the smooth random effect for cluster j . The model is fit using the `lme4`³⁶ and `rms` packages³⁷. This approach estimates the calibration per cluster and the variance of the random effects in a single step. As opposed to the random effects in 2MA-C, the MIX-C model takes all observations across the entire spectrum of predicted risk into account when predicting the realized values of the random effects and cluster-specific calibration curves. The main limitation is the computation time needed when the number of clusters is large. Illustrations are presented in **Supporting Material**

(Appendix A3, Figures S8-S9), code for the implementation is available in OSF repository (<https://osf.io/aj8ew/>).

2.7 RESULTS FOR THE CASE EXAMPLE

A visual analysis of the 3 curves shows that the three methods present similar results on the case example, in line with the previous obtained results ignoring clustering (Figure 3). All plots suggest that ADNEX overestimated risks. Nevertheless, there are important differences in the estimated uncertainty and heterogeneity, with 2MA-C having the narrowest confidence and prediction interval. Details, visualizations, and variations of each method are shown in Figures S2-S9.

3 SIMULATION STUDY

3.1 METHODS

The data generating models were based on logistic regression with a random intercept per cluster, hence the formula to obtain the true probabilities was of the form of $\text{logit}(\pi(x_{ij})) = \beta_0 + x_i\beta_1 + u_j$. β_0 represents the intercept, β_1 the effect of x_i and u_j is the cluster-specific deviation. We first obtain the true models according to a full factorial design where two factors were varied: little vs strong clustering (ICC 5% or 20%) and lower vs higher true AUC (0.75 and 0.9). Event rate was fixed at 30% for the whole population but varied between clusters. For each data generating mechanism, we generated data for 200 clusters and 2,000,000 patients (10,000 observations per cluster) and a single normally distributed linear predictor (x_i , which can be seen as a combination of several predictors) with mean 0 and variance 1. Random effects (u_j) were also normally distributed with variance according to the desired ICC. ICC is calculated as the variance of a null random intercept model divided by the total variance, calculated as the addition of the variances of the null random intercept model and the standard logistic distribution³⁸. AUC was controlled by varying the coefficient (β_1) and the desired event rate was controlled by modifying the intercept β_0 . We obtained 4 superpopulations by trial-error (Table S1). The code to obtain the superpopulations is available in OSF repository (<https://osf.io/aj8ew/>).

In each of the superpopulations we draw 4 scenarios, inspired by real validation studies, varying events per clusters (EPC) (20 vs 200) and number of clusters (5 vs 30). These scenarios refer to the dataset on which hypothetical prediction models are developed. This results in 16 scenarios overall, by combining all values for ICC, AUC, EPC and number of clusters. The clusters and patients within each cluster were selected randomly and the number of patients was selected according to the prevalence and the desired EPC ($n_j = \text{EPC} * 1.15$ divided by cluster prevalence, we multiply EPC to ensure that the desired EPC is obtained across all clusters). We developed logistic regression models with restricted cubic splines and 3 knots in these training datasets. Then, we externally validate the calibration of the model in patients from clusters not used for model development in an ideal situation with high number of centers and high EPC. Therefore, we validate models on a random selection of 100000 observations from a random selection of 30 clusters that were not sampled for model development. On average, each cluster contained 1000 events and 3333 observations, but the number of events varied depending on the cluster specific event rate.

We applied the CG-C (grouped and interval), 2MA-C (splines and loess) and MIX-C approaches to the validation sample. For comparison, we also obtained a standard flexible logistic calibration model (i.e. ignoring clustering) using restricted cubic splines and 3 knots. True risks are obtained using the formula in Table 2, and the true risks in the cluster with the average effect are obtained by setting the random intercept to 0. These true risks can be used to generate true calibration curves per cluster and for the

cluster with the average effect. To numerically compare the deviation of the estimated calibration curve from the true one, we calculate the mean squared calibration error (MSCE) as the mean squared difference between the estimated observed proportions and the true observed proportion (based on the true risks) in the cluster with the average effect (setting $u_j = 0$) over a fixed grid of 100 estimated risks (100 evenly spaced points from 0.01 to 0.99).²³ For CG-C, the grid contains 10 points by definition. The process was repeated 100 times per scenario, hence 16000 logistic regression models are developed and validated in 96.000 calibration models (6 approaches per model).

3.1.1 Heterogeneity

We evaluated the coverage of the 95% prediction intervals. For each of the three methods, using the same grid of values that we used for the MSCE, we evaluated whether the true cluster-specific risk (including random effects) falls within the prediction interval at each of the grid points. This means that we obtained the true cluster specific probabilities using the formula in **Table S1** and compare for each clustered calibration approach if the prediction interval contained the true values. Coverage was calculated for each of the 100 grid points.

3.2 RESULTS

The median MSCE results are displayed in **Table 2** (multiplied by 100) and **Figures 4** (subset of best approaches). Note that CG-C focuses on 10 points whereas the other approaches focus on a grid of 100 points, such that CG-C and the other approaches are not directly comparable. MIX-C, CG-C (grouped) and 2MA-C (splines) were the best performing approaches, with 2MA-C (splines) being the best performing model in 14 out of 16 scenarios. In the two scenarios with high ICC and high EPC, MIX-C performed best. Standard flexible logistic calibration performed considerably worse in all scenarios, in particular when ICC was high. Having more centers and having more events per center tended to slightly improve results, yet not for all approaches and not for all scenarios.

The mean pointwise coverage of the 95% prediction intervals was 95% for 2MA-C (splines) and CG-C (grouped), 94% for MIX-C, and 83% for 2MA-C (LOESS). However, the coverage differed along the estimated risks and across the different scenarios, with worse coverage in the tails for all methods (**Figure 5 and S10**). 2MA-C (splines) had close to nominal coverage for all scenarios except in the tail of the estimated risks and for the second superpopulation. MIX-C had low coverage (too narrow PI) for the first superpopulation and too wide intervals for the rest of the scenarios. In the second superpopulation, the coverage was poor when the estimated risks were higher than 50%, probably because there were few observations with risks in this range. CG-C (grouped) had close to nominal coverage except in the first quantiles of superpopulations with high AUC. CG-C (interval) only had correct prediction intervals with high AUC and low ICC. There was no method that had correct pointwise prediction interval coverage across all scenarios but all methods except CG-C (interval) were able to estimate prediction intervals around the prevalence (30%) when training sample size was high.

Code and data to reproduce the simulation study and analysis are available in **OSF repository** (<https://osf.io/aj8ew/>).

4 SYNTHETIC DATA

4.1 METHODS

To generate synthetic data, we use data from the International Ovarian Tumor Analysis (IOTA) consortium that was used to develop prediction models to estimate the risk of malignancy in patients with an ovarian tumor.^{9,25} We used the `synthpop` package in R, which learns the structure of the data and generates a new dataset where individual patient data is masked but the underlying structure is preserved.³⁹ We generated synthetic data for 1 million individuals for each of the 10 hospitals separately,

and use these synthetic patients cluster-specific populations (retaining the clustered structure of the original dataset). We generated two true models per center: one based on a logistic regression model with splines for continuous variables, and one based on a random forest model (with $mtry=3$ and minimum node size 10). Both models were trained on the real data from that center, using the nine ADNEX predictors listed above except type of center. The true models were applied to the 1 million synthetic patients, and the outcome was generated with Bernoulli trials based on the true risks of malignancy from the applied models. This means that the same synthetic patient has two true risks and can have two different outcomes. The code to generate the synthetic data is available in **OSF repository** (<https://osf.io/aj8ew/>), but the original data or the synthetic data are not publicly available. The comparison of the real and synthetic data for quality check in one center is presented in **Figure S11**.

We use the synthetic data to validate the calibration of the published ADNEX model without CA125 in each center.²⁵ We define 15 scenarios based on the number of centers (2,5,10) and validation data EPC (20,100,200,500,1000). We repeat this 1000 times, by randomly drawing validation datasets. If the number of centers is 2 or 5, the centers are randomly chosen as well. In each repetition, we calculate MSCE for the two true risks. True center-specific curves are obtained by training flexible calibration models (splines with 5 knots) on all 1 million synthetic patients from that center (**Figure 6**). We then compared the center specific estimated observed proportions and the true probabilities per center in a fixed grid of 100 values. The only method that obtains center specific curves accounting for clustering is the MIX-C method and we compare this to standard flexible calibration with LOESS and restricted cubic splines with 3 knots.

4.2 RESULTS

Median results for the synthetic data analysis with 1000 iterations are shown in **Table 3** and by center in **Figure 7**. MIX-C was the best performing method in all scenarios when the truth was based on a logistic regression with splines working as good in 5 scenarios. When the truth was based on a random forest model MIX-C was the best with small validation samples ($EPC < 500$) and loess when sample size was above 500 events per center. Additionally, the performance by approach varied considerably between centers (**Figure 7**). That is, the best approach varied by center.

5 DISCUSSION

Calibration of clinical prediction models is crucial since it is related to the usefulness of the recommended clinical decisions provided by the model.³ Evaluation of calibration performance is best done with flexible calibration plots.^{4,20} In this work, we introduced three methods for obtaining flexible calibration plots that account for clustering in the dataset. The first method extended the grouped calibration plot using bivariate random effects meta-analysis (CG-C method), the second method was a two-step approach in which flexible cluster-specific plots were combined through random effects meta-analysis. We generated cluster-specific plots in two ways: using restricted cubic splines (2MA-C splines) or LOESS (2MA-C loess). The third method used a mixed effects logistic calibration model using restricted cubic splines and random intercepts and slopes per cluster (MIX-C). Through a simulation study and a study using synthetic data from patients with an ovarian tumor, we observed MIX-C and 2MA-C (splines) worked best to obtain the calibration plot in the cluster with the average effect (simulation study) and MIX-C for the center specific calibration plots (synthetic data.) The coverage probability of the prediction interval was suboptimal for all methods and all scenarios with 2MA-C (Splines) standing out as the best across scenarios. A disadvantage of 2MA-C (Splines) is that the estimated calibration curves per center estimated with splines deviated more from the true curves per center than those obtained by MIX-C, which uses shrinkage to obtain better center-specific calibration curves. While CG-C may work well too to obtain a calibration plot in the cluster with the average effect

when using 10 groups based on deciles, it worked poorly when using 10 groups based on equal intervals of the estimated risk. The grouped approach tends to depend on the number and types of groups. Obviously, the other methods depend on the level of smoothing of the spline or LOESS method, but we selected automatically these parameters based on statistical goodness of fit to reduce the modeler's choices. We recommend using 2MA-C (splines) to estimate the curve with the average effect and the 95% PI and MIX-C for the cluster specific curves, specially when sample size per cluster is limited. We provide ready-to-use R functions to plot the curves and obtain numerical results in the OSF Repository (<https://osf.io/aj8ew/>), and they will soon be incorporated into the “CalibrationCurves” package in CRAN.⁴⁰

The main strength of our methodologies is the inclusion of a heterogeneity measure through the prediction intervals. These intervals indicate, for every estimated risk, the range within which the observed proportion may fall in a new cluster. It is crucial to differentiate the calibration in the cluster with the average effect with the cluster-specific calibration represented in the PIs. Whilst a model can be well calibrated in the cluster with the average effect, this does not necessarily imply that the model is perfectly calibrated in every individual cluster. Statements such as “the model was well calibrated” based on the cluster with the average effect calibration plot should be avoided, or at least accompanied by a clarification that this only applies to the summary curve. Using the interpretation of a calibration curve with the average effect for a specific cluster might lead to wrong decision making. For example, the curve with average effect suggests overestimation of risks but in some cluster the model might be underestimating them. Although no method provided prediction intervals with correct coverage in all investigated simulation scenarios (**Figure S10**) they show a more realistic picture than the cluster-ignorant confidence intervals. In general, all methods underestimate the heterogeneity between clusters therefore yielding too narrow prediction intervals, especially for estimated risks far from prevalence. Another limitation concerning CG-C and 2MA-C is that they present calibration plots based on meta-analysis of independent points. These approaches create the plot joining each pointwise estimate of observed proportion instead of creating a model for the whole plot and therefore are dependent on the number of points. Each of these points represents the calibration in the cluster with the average effect conditional on the estimated risks. We assume that all pointwise estimates form the calibration plot in the cluster with the average effect but in the modelling process each point is independent.

This study is a phase 2 methodological study that focused on the presentation of the methodology and assessments in a limited number of settings²⁴. Further research should therefore evaluate the methods in more extended settings and applications. For example, simulations could focus on more complex truths, such as multiple predictors with random slopes for their effects on the outcome, continuous predictors with nonlinear associations with the outcome under study, and prediction models based on flexible machine learning methods such as random forests, boosting approaches, or neural networks. Furthermore, our simulation study focused on model validation in an ideal setting with a large number of centers and a large number of outcome events per center. Future work should include different validation settings, including less ideal settings that are often seen in applied studies. Instead of performing a larger simulation study, we decided to focus on synthetic data based on real data from 10 hospitals on women with an ovarian tumor with the aim of building diagnostic prediction models to estimate the risk of malignancy. This data was used to evaluate an existing prediction model, ADNEX, which was a multinomial logistic regression model using random intercepts and uniform shrinkage of model coefficients.²⁵ In this synthetic data analysis we focused on the center specific performance of MIX-C varying the validation sample. MIX-C showed good results especially when sample size is limited where non-clustered approaches worked worse in general.

Another area of future research could focus on finetuning the methods such that they can work with other flexible calibration approaches such as kernel density based plots or other spline functions than the restricted cubic splines used in this work.

AUTHOR CONTRIBUTIONS

Contributions were based on the CRediT taxonomy. Conceptualization: LB, LW, BVC. Funding acquisition: LW, BVC. Project administration: LB. Supervision: LW, BVC. Methodology: LB, LW, BVC, BDCC. Resources: LB. Investigation: LB, LW, BVC. Validation: LB, LW, BVC, BDCC. Data curation: BVC. Software: LB. Formal analysis: LB, LW, BVC. Visualization: LB, LW, BVC. Writing – original draft: LB, LW, BVC. Writing – review & editing: LB, LW, BVC, BDCC. All authors have read, share final responsibility for the decision to submit for publication, and agree to be accountable for all aspects of the work.

DATA AVAILABILITY

Data and code to reproduce results and figures are available in a public, open access repository (link <https://osf.io/aj8ew/>). All data relevant to the study are included in the article or uploaded as supplementary information except the motivating example data and the synthetic data due to privacy concerns.

ACKNOWLEDGMENTS

FUNDING INFORMATION

This research was supported by the Research Foundation – Flanders (FWO) under grant G097322N with BVC as supervisors. LW and BVC were supported by Internal Funds KU Leuven (grant C24M/20/064). LB is supported by a long stay abroad grant from Research Foundation – Flanders (FWO) under grant V457024N.

CONFLICT OF INTEREST STATEMENT

The authors declare that there is no conflict of interest.

6 REFERENCES

1. Steyerberg EW. *Clinical Prediction Models: A Practical Approach to Development, Validation, and Updating*. Cham: Springer International Publishing; 2019. doi:10.1007/978-3-030-16399-0
2. van Smeden M, Reitsma JB, Riley RD, Collins GS, Moons KG. Clinical prediction models: diagnosis versus prognosis. *Journal of Clinical Epidemiology*. 2021;132:142-145. doi:10.1016/j.jclinepi.2021.01.009
3. Van Calster B, Vickers AJ. Calibration of Risk Prediction Models: Impact on Decision-Analytic Performance. *Med Decis Making*. 2015;35(2):162-169. doi:10.1177/0272989X14547233
4. Van Calster B, Nieboer D, Vergouwe Y, De Cock B, Pencina MJ, Steyerberg EW. A calibration hierarchy for risk models was defined: from utopia to empirical data. *Journal of Clinical Epidemiology*. 2016;74:167-176. doi:10.1016/j.jclinepi.2015.12.005
5. Riley RD, Stewart LA, Tierney JF. Individual Participant Data Meta-Analysis for Healthcare Research. In: *Individual Participant Data Meta-Analysis*. John Wiley & Sons, Ltd; 2021:1-6. doi:10.1002/9781119333784.ch1
6. Wynants L, Kent DM, Timmerman D, Lundquist CM, Van Calster B. Untapped potential of multicenter studies: a review of cardiovascular risk prediction models revealed inappropriate analyses and wide variation in reporting. *Diagn Progn Res*. 2019;3:6. doi:10.1186/s41512-019-0046-9
7. Wessler BS, Paulus J, Lundquist CM, et al. Tufts PACE Clinical Predictive Model Registry: update 1990 through 2015. *Diagnostic and Prognostic Research*. 2017;1(1):20. doi:10.1186/s41512-017-0021-2
8. Debray TPA, Collins GS, Riley RD, et al. Transparent reporting of multivariable prediction models developed or validated using clustered data: TRIPOD-Cluster checklist. *BMJ*. 2023;380:e071018. doi:10.1136/bmj-2022-071018
9. Van Calster B, Valentin L, Froyman W, et al. Validation of models to diagnose ovarian cancer in patients managed surgically or conservatively: multicentre cohort study. *BMJ*. 2020;370:m2614. doi:10.1136/bmj.m2614
10. Gupta RK, Harrison EM, Ho A, et al. Development and validation of the ISARIC 4C Deterioration model for adults hospitalised with COVID-19: a prospective cohort study. *Lancet Respir Med*. 2021;9(4):349-359. doi:10.1016/S2213-2600(20)30559-2
11. Steyerberg EW, Nieboer D, Debray TPA, van Houwelingen HC. Assessment of heterogeneity in an individual participant data meta-analysis of prediction models: An overview and illustration. *Stat Med*. 2019;38(22):4290-4309. doi:10.1002/sim.8296
12. Amsterdam WAC van. A causal viewpoint on prediction model performance under changes in case-mix: discrimination and calibration respond differently for prognosis and diagnosis predictions. September 2024. <http://arxiv.org/abs/2409.01444>. Accessed October 16, 2024.
13. Wynants L, Vergouwe Y, Van Huffel S, Timmerman D, Van Calster B. Does ignoring clustering in multicenter data influence the performance of prediction models? A simulation study. *Stat Methods Med Res*. 2018;27(6):1723-1736. doi:10.1177/0962280216668555

14. Debray TPA, Moons KGM, Ahmed I, Koffijberg H, Riley RD. A framework for developing, implementing, and evaluating clinical prediction models in an individual participant data meta-analysis. *Statistics in Medicine*. 2013;32(18):3158-3180. doi:10.1002/sim.5732
15. de Jong VMT, Moons KGM, Eijkemans MJC, Riley RD, Debray TPA. Developing more generalizable prediction models from pooled studies and large clustered data sets. *Statistics in Medicine*. 2021;40(15):3533-3559. doi:10.1002/sim.8981
16. Moher D, Schulz KF, Simera I, Altman DG. Guidance for Developers of Health Research Reporting Guidelines. *PLoS Med*. 2010;7(2):e1000217. doi:10.1371/journal.pmed.1000217
17. Snijders TAB, Bosker RJ. *Multilevel Analysis: An Introduction to Basic and Advanced Multilevel Modeling*. London, England, United Kingdom: Sage Publishers; 2012.
18. Finch WH, Bolin JE, Kelley K. *Multilevel Modeling Using R*. 2nd ed. New York: Chapman and Hall/CRC; 2019. doi:10.1201/9781351062268
19. Calster BV, Collins GS, Vickers AJ, et al. Performance evaluation of predictive AI models to support medical decisions: Overview and guidance. December 2024. doi:10.48550/arXiv.2412.10288
20. Austin PC, Steyerberg EW. Graphical assessment of internal and external calibration of logistic regression models by using loess smoothers. *Statistics in Medicine*. 2014;33(3):517-535. doi:10.1002/sim.5941
21. Austin PC, Harrell FE, Van Klaveren D. Graphical calibration curves and the integrated calibration index (ICI) for survival models. *Statistics in Medicine*. 2020;39(21):2714-2742. doi:10.1002/sim.8570
22. Austin PC, Putter H, Giardiello D, van Klaveren D. Graphical calibration curves and the integrated calibration index (ICI) for competing risk models. *Diagn Progn Res*. 2022;6(1):2. doi:10.1186/s41512-021-00114-6
23. Van Hoorde K, Van Huffel S, Timmerman D, Bourne T, Van Calster B. A spline-based tool to assess and visualize the calibration of multiclass risk predictions. *Journal of Biomedical Informatics*. 2015. doi:10.1016/j.jbi.2014.12.016
24. Heinze G, Boulesteix AL, Kammer M, Morris TP, White IR, Initiative the SP of the S. Phases of methodological research in biostatistics—Building the evidence base for new methods. *Biometrical Journal*. 2024;66(1):2200222. doi:10.1002/bimj.202200222
25. Van Calster B, Hoorde KV, Valentin L, et al. Evaluating the risk of ovarian cancer before surgery using the ADNEX model to differentiate between benign, borderline, early and advanced stage invasive, and secondary metastatic tumours: prospective multicentre diagnostic study. *BMJ*. 2014;349:g5920. doi:10.1136/bmj.g5920
26. Timmerman D, Ledger A, Bourne T, et al. IOTA Phase 1: development of models to distinguish between a benign and malignant adnexal tumor before surgery. February 2024. doi:10.48804/HDFDWI
27. Kaijser J. Towards an evidence-based approach for diagnosis and management of adnexal masses: findings of the International Ovarian Tumour Analysis (IOTA) studies. *Facts Views Vis Obgyn*. 2015;7(1):42-59.
28. Dimitriadis T, Dümbgen L, Henzi A, Puke M, Ziegel J. Honest calibration assessment for binary outcome predictions. *Biometrika*. 2023;110(3):663-680. doi:10.1093/biomet/asac068

29. Campo BDC. Towards reliable predictive analytics: a generalized calibration framework. September 2023. doi:10.48550/arXiv.2309.08559
30. On behalf of Topic Group ‘Evaluating diagnostic tests and prediction models’ of the STRATOS initiative, Van Calster B, McLernon DJ, van Smeden M, Wynants L, Steyerberg EW. Calibration: the Achilles heel of predictive analytics. *BMC Med.* 2019;17(1):230. doi:10.1186/s12916-019-1466-7
31. Cox DR. Two Further Applications of a Model for Binary Regression. *Biometrika.* 1958;45(3/4):562-565. doi:10.2307/2333203
32. Harrell , FE. *Regression Modeling Strategies: With Applications to Linear Models, Logistic and Ordinal Regression, and Survival Analysis.* Cham: Springer International Publishing; 2015. doi:10.1007/978-3-319-19425-7
33. Wickham H, Averick M, Bryan J, et al. Welcome to the tidyverse. *Journal of Open Source Software.* 2019;4(43):1686. doi:10.21105/joss.01686
34. Viechtbauer W. Conducting Meta-Analyses in R with the metafor Package. *Journal of Statistical Software.* 2010;36:1-48. doi:10.18637/jss.v036.i03
35. Barreñada L, Wynants L, Calster B van. Clustered Flexible Calibration Plots For Binary Outcomes Using Random Effects Modeling. July 2024. <https://osf.io/erju9/>. Accessed March 11, 2025.
36. Bates D, Mächler M, Bolker B, Walker S. Fitting Linear Mixed-Effects Models Using **lme4**. *J Stat Soft.* 2015;67(1). doi:10.18637/jss.v067.i01
37. Harrell Jr FE. rms: Regression Modeling Strategies. September 2009:7.0-0. doi:10.32614/CRAN.package.rms
38. Hosmer DW, Lemeshow S, Sturdivant RX. *Applied Logistic Regression.* 1st ed. Wiley; 2013. doi:10.1002/9781118548387
39. Nowok B, Raab GM, Dibben C. synthpop: Bespoke Creation of Synthetic Data in R. *Journal of Statistical Software.* 2016;74:1-26. doi:10.18637/jss.v074.i11
40. De Cock B, Nieboer D, Van Calster B, Steyerberg EW, Vergouwe Y. The CalibrationCurves package: assessing the agreement between observed outcomes and predictions. 2023. doi:10.32614/CRAN.package.CalibrationCurves
41. van Houwelingen HC, Arends LR, Stijnen T. Advanced methods in meta-analysis: multivariate approach and meta-regression. *Stat Med.* 2002;21(4):589-624. doi:10.1002/sim.1040
42. Berkey CS, Hoaglin DC, Mosteller F, Colditz GA. A random-effects regression model for meta-analysis. *Stat Med.* 1995;14(4):395-411. doi:10.1002/sim.4780140406
43. Reitsma JB, Glas AS, Rutjes AWS, Scholten RJPM, Bossuyt PM, Zwinderman AH. Bivariate analysis of sensitivity and specificity produces informative summary measures in diagnostic reviews. *J Clin Epidemiol.* 2005;58(10):982-990. doi:10.1016/j.jclinepi.2005.02.022
44. Riley RD, Higgins JPT, Deeks JJ. Interpretation of random effects meta-analyses. *BMJ.* 2011;342:d549. doi:10.1136/bmj.d549
45. Veroniki AA, Jackson D, Viechtbauer W, et al. Methods to estimate the between-study variance and its uncertainty in meta-analysis. *Res Synth Methods.* 2016;7(1):55-79. doi:10.1002/jrsm.1164

46. Schwarzer G, Carpenter JR, Rücker G. *Meta-Analysis with R*. Cham: Springer International Publishing; 2015. doi:10.1007/978-3-319-21416-0
47. Snell KI, Ensor J, Debray TP, Moons KG, Riley RD. Meta-analysis of prediction model performance across multiple studies: Which scale helps ensure between-study normality for the C-statistic and calibration measures? *Stat Methods Med Res*. 2018;27(11):3505-3522. doi:10.1177/0962280217705678
48. Higgins JPT, Thompson SG, Spiegelhalter DJ. A re-evaluation of random-effects meta-analysis. *J R Stat Soc Ser A Stat Soc*. 2009;172(1):137-159. doi:10.1111/j.1467-985X.2008.00552.x
49. Partlett C, Riley RD. Random effects meta-analysis: Coverage performance of 95% confidence and prediction intervals following REML estimation. *Stat Med*. 2017;36(2):301-317. doi:10.1002/sim.7140
50. Nagashima K, Noma H, Furukawa TA. Prediction intervals for random-effects meta-analysis: A confidence distribution approach. *Stat Methods Med Res*. 2019;28(6):1689-1702. doi:10.1177/0962280218773520
51. Skipka G. The inclusion of the estimated inter-study variation into forest plots for random effects meta-analyses – a suggestion for a graphical representation. <https://abstracts.cochrane.org/2006-dublin/inclusion-estimated-inter-study-variation-forest-plots-random-effects-meta-analyses>. Published 2006.

Figures

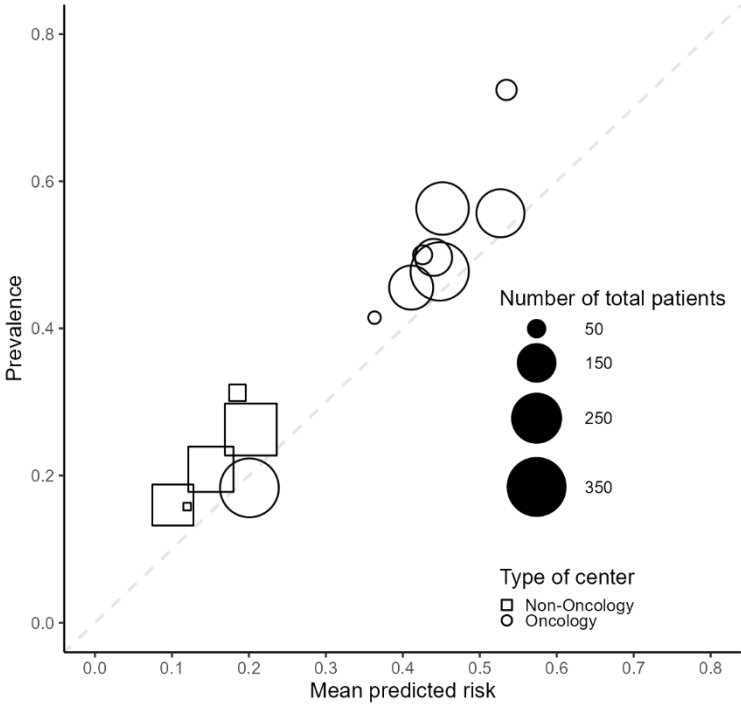


Figure 1. Prevalence and mean predicted ADNEX risk by center across the 14 centers in the dataset.

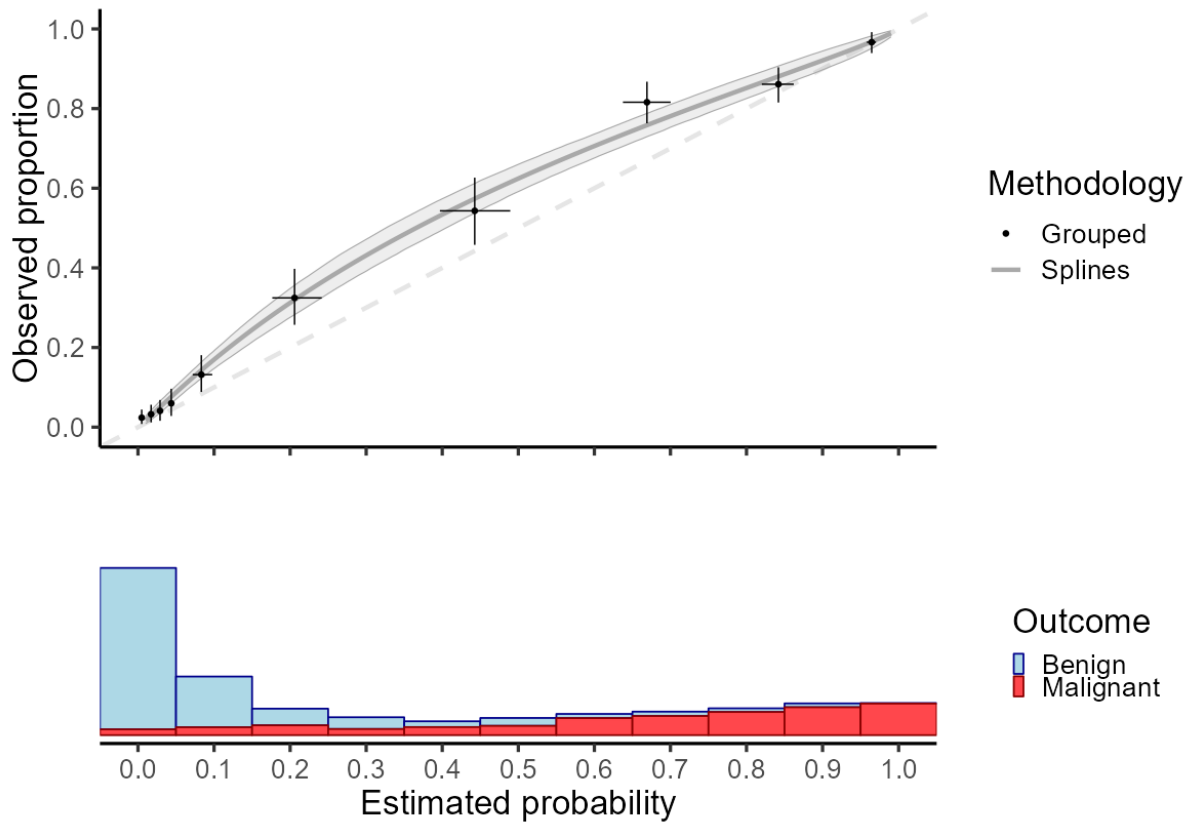


Figure 2. Traditional flexible calibration curves. Observed proportion is estimated with a logistic model with restricted cubic splines to model nonlinear effects and estimated risks are grouped in 10 groups. Confidence intervals are shown for 1000 bootstraps.

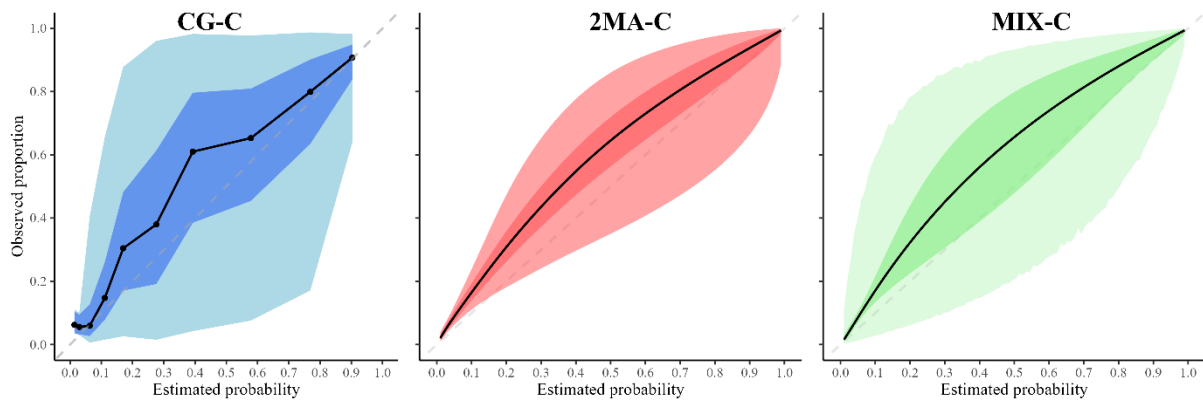


Figure 3. Comparison of the 3 introduced methodologies with confidence and prediction intervals. Number of quantiles for CG-C were 10, 2MA-C pooled center specific curves with splines and MIX-C used random intercept and slopes with restricted cubic splines and 3 knots.

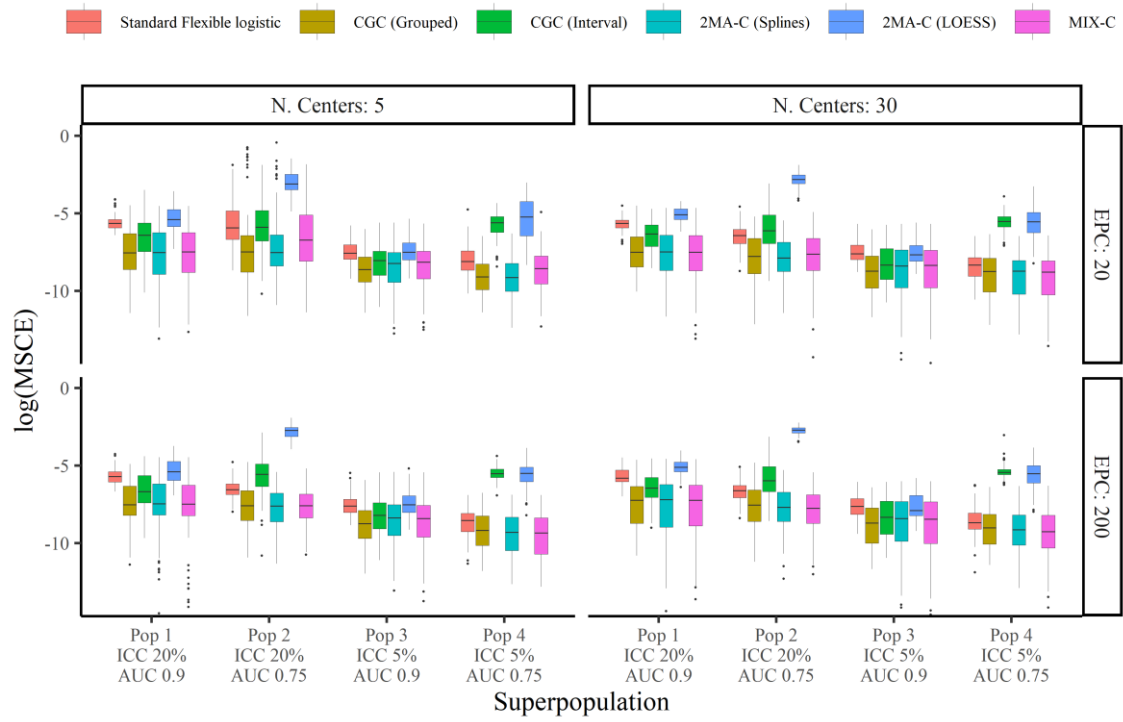


Figure 4. Boxplots of mean squared calibration error (log) for the prediction model based on standard logistic regression. Standard flexible logistic calibration is obtained by fitting a model with restricted cubic splines and three knots in the pooled data from all centers.

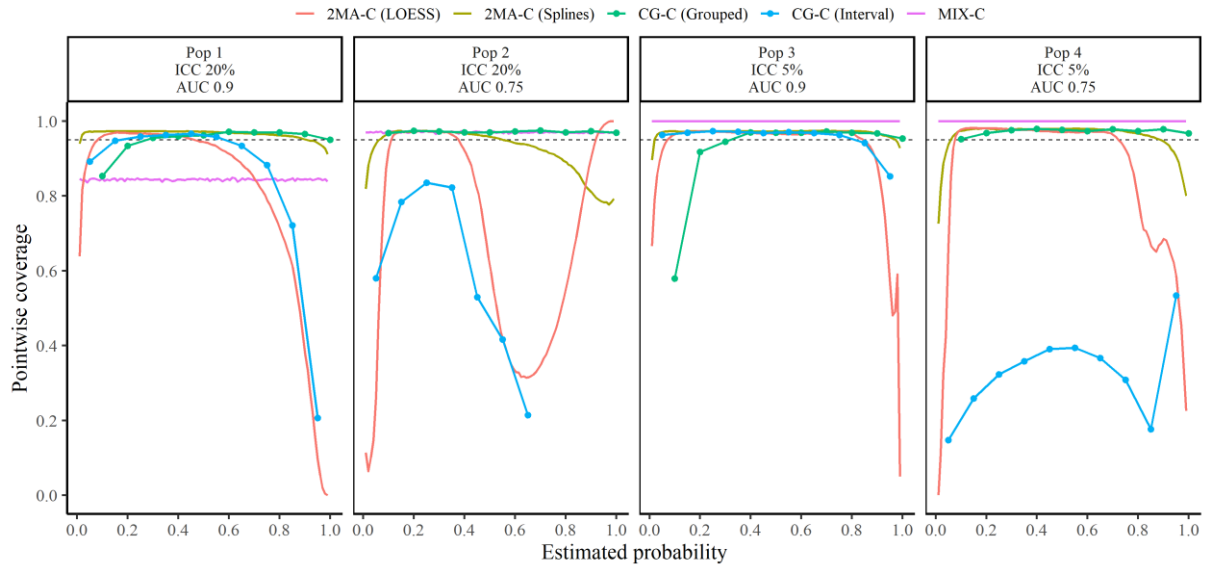


Figure 5. Pointwise heterogeneity average coverage for logistic regression models trained in datasets of 30 centers and 200 events per center. Black dotted line indicates nominal coverage (95%)

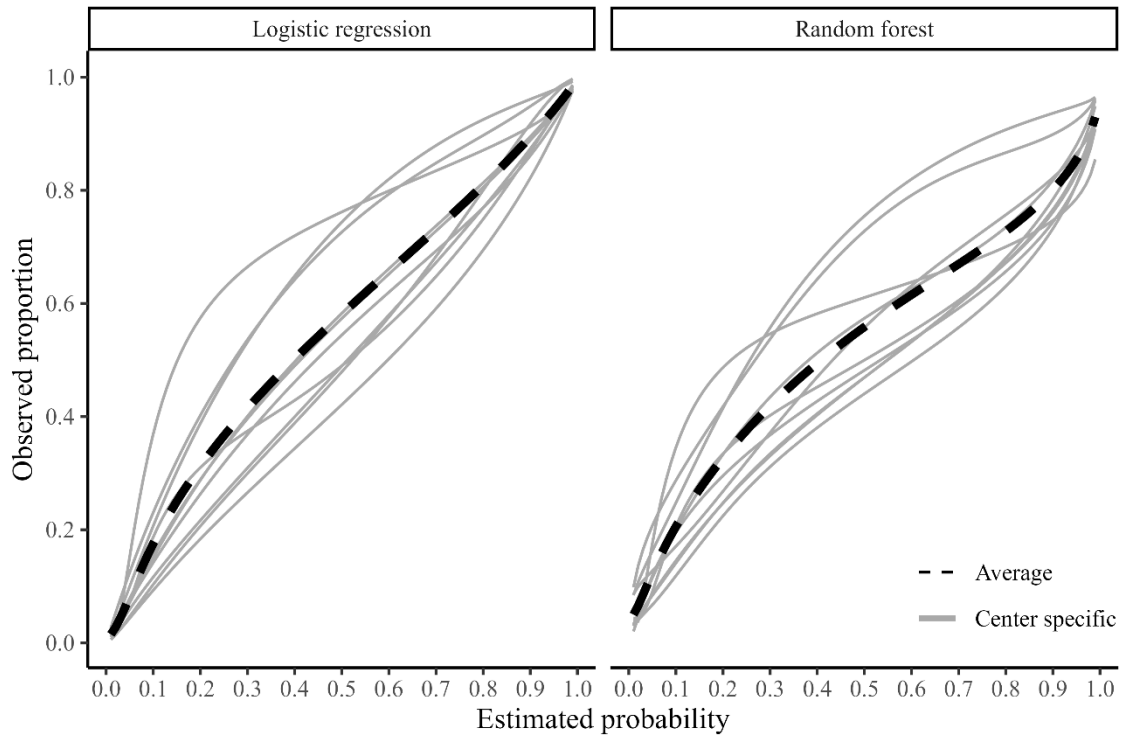


Figure 6. Center specific (grey) and average true calibration plots for the synthetic data with 1000000 observations per center.

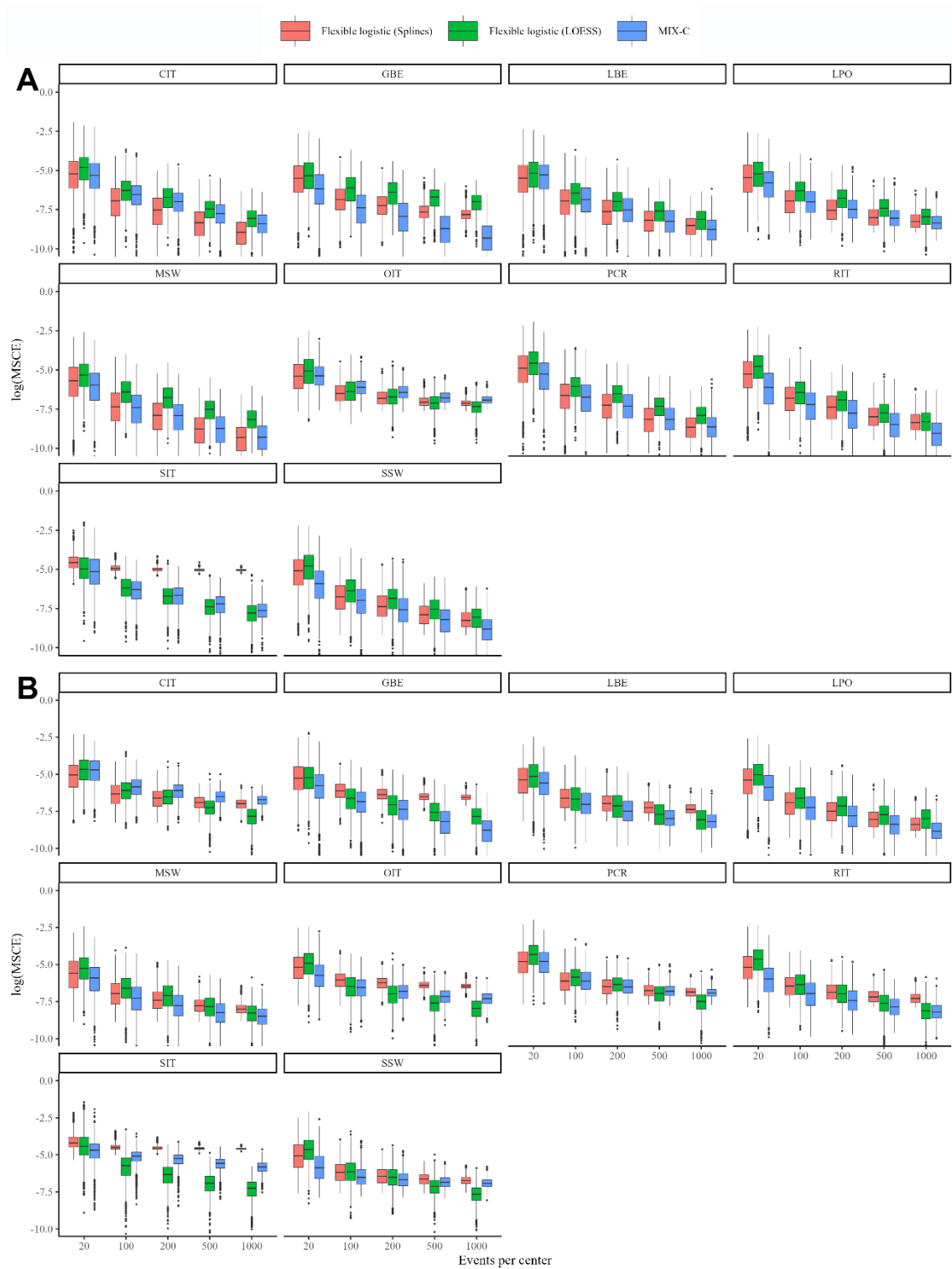


Figure 7. Center specific results of MSCE (multiplied by 100) by the number of events per center for the logistic truth (A) and the random forest (B) truth.

Tables

Method	Estimation of observed proportion	Strengths	Limitations	Implementation	Illustration
CG-C	<p>Grouped: Bivariate random effects meta-analysis of logit-transformed mean estimated risk and event fraction by quantile per cluster.</p> <p>Interval: Bivariate random effects meta-analysis of logit-transformed mean estimated risk and event fraction by estimated risk interval.</p>	<p>Model agnostic</p> <p>Pointwise confidence and prediction intervals.</p> <p>All clusters have the same number of groups</p>	<p>Computation time</p> <p>Groups can contain observations with very different estimated risks within and between clusters (Grouped version).</p> <p>Clusters may not have the same number of groups (e.g. risk intervals without observations). (Interval version)</p> <p>Curves depend on number of groups</p>	<p>CGC(method = "grouped")</p> <p>CGC(method = "interval")</p>	<p>Figures S2-3</p> <p>Figures S4-S5</p>
2MA-C	<p>Random effects meta-analysis of estimated smooth observed proportion by cluster</p> <p>Splines: Recommended when clusters are small</p> <p>LOESS: More flexible but can fail with small clusters.</p>	<p>Pointwise confidence and prediction intervals.</p>	<p>Computation time</p> <p>Curve dependent on the smoother used in the cluster-specific models.</p>	<p>MAC2(method_choi = "splines")</p> <p>MAC2(method_choi = "loess")</p>	<p>Figure S6 (Splines)</p> <p>Figure S7 (LOESS)</p>
MIX-C	<p>Logistic generalized linear mixed model with restricted cubic splines.</p>	<p>Curvewise confidence and prediction intervals.</p> <p>Provides also shrunken curves per center.</p>	<p>Computation time</p>	<p>MIXC(model = "intercept")</p> <p>MIXC(model = "slope")</p>	<p>Figure S8 (intercept)</p> <p>Figure S9 (slope)</p>

Table 1. Overview of introduced methodologies for creating flexible calibration curves accounting for clustering.

Table 2. Median (IQR) difference between true average probabilities and estimated observed proportion with logistic calibration, CG-C (10 groups) ,2MA-C and MIX-C method for a logistic model. Multiplied by 100. The lower the number, the closer the estimated summary calibration curve is to the true calibration curve in a cluster with an average effect.

EPC	N. Cent	ICC	AUC	Satndard Flexible Logistic	CG-C group*	CG-C interval*	2MA-C Splines	2MA-C LOESS	MIX-C
20	5	0.05	0.75	0.03 (0.02-0.06)	0.01 (0.00-0.03)	0.51 (0.27-0.70)	0.01 (0.00-0.03)	0.54 (0.16-1.45)	0.02 (0.01-0.04)
20	5	0.05	0.9	0.05 (0.04-0.09)	0.02 (0.01-0.04)	0.03 (0.01-0.06)	0.03 (0.01-0.05)	0.06 (0.03-0.10)	0.03 (0.01-0.06)
20	5	0.2	0.75	0.27 (0.13-0.80)	0.06 (0.02-0.16)	1.13 (0.56-2.07)	0.06 (0.02-0.17)	4.54 (3.13-8.44)	0.12 (0.03-0.61)
20	5	0.2	0.9	0.36 (0.27-0.46)	0.05 (0.02-0.18)	0.17 (0.06-0.36)	0.06 (0.01-0.20)	0.46 (0.29-0.87)	0.06 (0.02-0.20)
20	30	0.05	0.75	0.02 (0.01-0.04)	0.02 (0.00-0.04)	0.47 (0.33-0.59)	0.02 (0.00-0.03)	0.40 (0.20-0.72)	0.02 (0.00-0.03)
20	30	0.05	0.9	0.05 (0.03-0.09)	0.02 (0.01-0.04)	0.02 (0.01-0.07)	0.02 (0.01-0.07)	0.05 (0.03-0.09)	0.02 (0.01-0.06)
20	30	0.2	0.75	0.16 (0.10-0.24)	0.04 (0.01-0.14)	1.15 (0.72-1.75)	0.04 (0.02-0.11)	6.06 (4.61-8.15)	0.05 (0.02-0.13)
20	30	0.2	0.9	0.36 (0.27-0.44)	0.06 (0.02-0.15)	0.18 (0.08-0.32)	0.06 (0.02-0.17)	0.63 (0.46-0.91)	0.06 (0.02-0.16)
200	5	0.05	0.75	0.02 (0.01-0.03)	0.01 (0.00-0.03)	0.42 (0.34-0.58)	0.01 (0.00-0.02)	0.41 (0.24-0.61)	0.01 (0.00-0.02)
200	5	0.05	0.9	0.05 (0.03-0.08)	0.02 (0.01-0.04)	0.03 (0.01-0.06)	0.02 (0.01-0.05)	0.05 (0.03-0.10)	0.02 (0.01-0.05)
200	5	0.2	0.75	0.14 (0.10-0.21)	0.05 (0.02-0.13)	1.23 (0.64-2.03)	0.05 (0.02-0.11)	6.55 (4.45-7.90)	0.05 (0.02-0.11)
200	5	0.2	0.9	0.34 (0.24-0.46)	0.06 (0.03-0.18)	0.13 (0.06-0.36)	0.06 (0.03-0.21)	0.46 (0.26-0.90)	0.06 (0.03-0.19)
200	30	0.05	0.75	0.02 (0.01-0.03)	0.01 (0.00-0.03)	0.44 (0.38-0.54)	0.01 (0.00-0.03)	0.41 (0.22-0.68)	0.01 (0.00-0.03)
200	30	0.05	0.9	0.05 (0.03-0.08)	0.02 (0.00-0.04)	0.02 (0.01-0.07)	0.02 (0.01-0.07)	0.04 (0.03-0.10)	0.02 (0.00-0.07)
200	30	0.2	0.75	0.13 (0.09-0.19)	0.05 (0.02-0.14)	1.17 (0.62-2.05)	0.05 (0.02-0.12)	6.71 (5.57-7.72)	0.04 (0.02-0.10)
200	30	0.2	0.9	0.31 (0.24-0.51)	0.07 (0.02-0.18)	0.16 (0.09-0.32)	0.08 (0.01-0.20)	0.62 (0.46-0.85)	0.07 (0.01-0.19)

*Deciles is calculated only with 10 points instead of 100. In green the best working model(s) for estimating observed proportions excluding CG-C methods.

Table 3. Median MSCE for the synthetic data study for center specific results. MSCE is presented multiplied by 100. Note that the center specific true curves are based on a flexible logistic model with restricted cubic splines. The lower the number, the closer the estimated center-specific calibration curve is to the true calibration curve in each cluster.

EPC	N. centers	Logistic regression truth			Random forest truth		
		Flexible logistic (Splines)	Flexible logistic (LOESS)	MIX-C	Flexible logistic (Splines)	Flexible logistic (LOESS)	MIX-C
20	2	0.54 (0.21-1.11)	0.66 (0.29-1.37)	0.52 (0.23-1.01)	0.65 (0.28-1.38)	0.81 (0.39-1.63)	0.58 (0.25-1.19)
20	5	0.57 (0.22-1.19)	0.68 (0.30-1.43)	0.39 (0.15-0.85)	0.66 (0.26-1.31)	0.83 (0.39-1.63)	0.44 (0.19-0.96)
20	10	0.55 (0.22-1.13)	0.67 (0.3-1.41)	0.33 (0.13-0.72)	0.64 (0.27-1.31)	0.81 (0.38-1.62)	0.38 (0.16-0.85)
100	2	0.13 (0.06-0.29)	0.19 (0.10-0.36)	0.13 (0.06-0.27)	0.19 (0.10-0.38)	0.19 (0.09-0.35)	0.17 (0.08-0.35)
100	5	0.13 (0.05-0.28)	0.18 (0.09-0.34)	0.12 (0.05-0.23)	0.19 (0.10-0.39)	0.19 (0.09-0.36)	0.15 (0.07-0.32)
100	10	0.13 (0.06-0.28)	0.18 (0.09-0.34)	0.11 (0.04-0.22)	0.20 (0.10-0.38)	0.18 (0.09-0.35)	0.14 (0.06-0.30)
200	2	0.08 (0.03-0.15)	0.11 (0.06-0.21)	0.08 (0.03-0.15)	0.14 (0.08-0.25)	0.12 (0.06-0.20)	0.11 (0.05-0.23)
200	5	0.07 (0.03-0.16)	0.12 (0.07-0.21)	0.07 (0.03-0.14)	0.14 (0.08-0.25)	0.12 (0.06-0.20)	0.10 (0.05-0.21)
200	10	0.07 (0.03-0.16)	0.12 (0.06-0.21)	0.07 (0.03-0.13)	0.14 (0.07-0.25)	0.11 (0.06-0.20)	0.10 (0.04-0.20)
500	2	0.04 (0.02-0.08)	0.06 (0.03-0.11)	0.04 (0.02-0.08)	0.11 (0.06-0.18)	0.06 (0.03-0.11)	0.07 (0.03-0.13)
500	5	0.04 (0.02-0.08)	0.06 (0.03-0.11)	0.03 (0.02-0.07)	0.11 (0.06-0.17)	0.06 (0.03-0.11)	0.07 (0.03-0.13)
500	10	0.04 (0.02-0.08)	0.06 (0.03-0.11)	0.03 (0.01-0.07)	0.11 (0.06-0.17)	0.06 (0.03-0.11)	0.07 (0.03-0.13)
1000	2	0.03 (0.01-0.06)	0.04 (0.02-0.06)	0.02 (0.01-0.05)	0.10 (0.05-0.15)	0.04 (0.02-0.06)	0.05 (0.02-0.11)
1000	5	0.03 (0.01-0.06)	0.04 (0.02-0.07)	0.02 (0.01-0.04)	0.10 (0.05-0.15)	0.04 (0.02-0.07)	0.06 (0.02-0.11)
1000	10	0.03 (0.01-0.06)	0.04 (0.02-0.07)	0.02 (0.01-0.04)	0.10 (0.05-0.15)	0.04 (0.02-0.07)	0.06 (0.02-0.11)

APPENDIX

A1. CLUSTERED GROUP CALIBRATION (CG-C)

Clustered group calibration can be seen as an extension of the traditional grouped calibration or binning calibration where the data is split into equally sized groups based on the distribution of estimated risks and the calibration curve shows for each group the estimated prevalence of the event on the y-axis and the mean estimated risks on the x-axis.

CG-C (grouped)

1. For each cluster $j = (1, \dots, J)$, we group the estimated probabilities in Q quantiles. Quantiles typically differ by cluster.
2. In each quantile q , we calculate the mean outcome \bar{y}_{qj} , the mean predicted probability $\bar{\hat{\pi}}_{qj}$ and the number of observations in each quantile n_{qj} for each cluster j .
3. To obtain the pooled estimated risk and observed proportion, we perform a random effects bivariate meta-analysis using the logit-transformed \bar{y}_{qj} and $\bar{\hat{\pi}}_{qj}$. We use an unstructured covariance matrix⁴¹⁻⁴³ and estimate both the within- and between-cluster heterogeneity.

Using the fitted model, we estimate the observed proportion and estimated risk of cluster j in quantile q . The variance of the random effects (between cluster variability) as well as the sampling error (within cluster variability) are captured by the covariance matrices. To fit the model, we utilize the `rma.mv` function of the `metafor` package with `cluster` as the grouping factor and an unstructured variance-covariance matrix (see <https://wviechtb.github.io/metafor/reference/rma.mv.html> for a comprehensive overview). Confidence intervals are obtained with profile likelihood and prediction intervals calculated as explained by Riley and colleagues.⁴⁴

CG-C (interval)

The algorithm is the same as CG-C (grouped) but in step 1 instead of grouping based on quantiles we create Q intervals evenly dividing the probability space (0-1). Then steps 2 and 3 are identical.

A2. TWO STAGE META-ANALYSIS (2MA-C)

The two stage meta-analysis approach combines individual cluster specific calibration models to obtain the calibration in the cluster with the average effect. The process has two stages, first obtaining the individual cluster's calibration and then combining them using random effects meta-analysis as follows:

Stage 1

Fit a flexible calibration model (LOESS or splines) per cluster and estimate observed proportion for a grid of values (e.g. 100 values from 0.01 to 0.99)

We estimate for a grid (X) of values from 0.01 to 0.99 the corresponding observed proportion with the calibration model.

Stage 2

Pool observed proportion per grid value (x) using a random effects model:

$$\text{logit}({}_s\hat{\pi}_{ij}) = \hat{\pi}\mu_i + v_{ij} + \epsilon_{ij}, \quad \epsilon_{ij} \sim N(0, \sigma_{ij}^2), \quad v_{ij} \sim N(0, \tau_i^2)$$

With $\text{logit}({}_s\hat{\pi}_{ij})$ the logit-transformed predicted probability for point i within cluster j , v_{ij} the random effect of cluster j and ϵ_{ij} the error term. The summary estimate is obtained using inverse variance weighting.

$$\text{logit}({}_s\hat{\pi}_i) = \frac{\sum_{j=1}^N \text{logit}({}_s\hat{\pi}_{ij}) w_{ij}}{\sum_{j=1}^N w_{ij}}$$

where w_{ij} denote the weights calculated as

$$w_{ij} = \frac{1}{\tau_i^2 + \sigma_{ij}^2}.$$

τ_i^2 is the between cluster variability or heterogeneity estimated with REML (see Veroniki et al. for an overview of methods to estimate τ_i^2 ⁴⁵) in point i and σ_{ij} is the within cluster standard error of point i in cluster j .

The confidence interval can be calculated using the HKSJ approach, which is recommended when the number of studies is small^{46,47} or with the default method.

Finally we get prediction interval based on the t-distribution as explained in Higgins et al (2009)

$\text{logit}({}_s\hat{\pi}_{ij}) \mp t_{j-2} \sqrt{\tau_i^2 + SE(\text{logit}({}_s\hat{\pi}_{ij}))^2}$ ⁴⁸ (default) where t_{j-2} denotes the t- student distribution with $j-2$ degrees of freedom or any of the supported methods for `meta` package, namely Harktung-Knapp, Kenward Roger⁴⁹, bootstrap approach⁵⁰ or based on standard normal quantile⁵¹.

A3. ONE STEP MIXED MODEL (MIX-C)

This approach estimates confidence intervals as:

$$\text{logit}\left(\text{P}(y_{ij} = 1 \mid \hat{\pi}(x_{ij}), \tilde{s}_j)\right) \mp z_{1-\frac{\alpha}{2}} \text{SE}\left(\text{logit}\left(\text{P}(y_{ij} = 1 \mid \hat{\pi}(x_{ij}), \tilde{s}_j)\right)\right)$$

With $z_{1-\frac{\alpha}{2}}$ representing the quantile of the standard normal distribution that corresponds to the cumulative probability of $1 - \frac{\alpha}{2}$ (i.e. 1.96 for a 95% CI). Prediction intervals are calculated using the `predictInterval` function in R with 10 000 samples (simulation based). This function takes into account the uncertainty at observation level (residual variance), in the fixed coefficients and in the random effects. In this method we first obtain the random and fixed effects, then we generate n samples (default = 10000) based on a multinomial normal distribution of the random and fixed effects, separately. Then we calculate the linear predictor in each sample and predict the upper and lower limits of prediction interval.

A4. FIGURES

Supplementary Figure 9. Centre-specific calibration curves of Assessment of Different NEoplasias in the adneXa (ADNEX) without CA125. "Other" includes the following small non-oncology centres with low prevalence of malignancy: London and Nottingham from the UK, and Milan 3 and Florence from Italy.

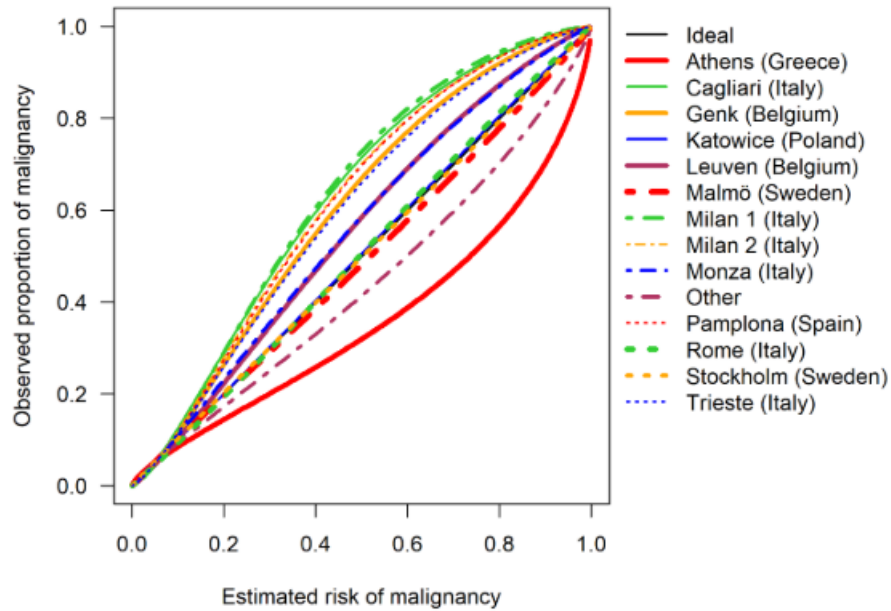


Figure S1. ADNEX without CA125 center specific logistic calibration curves in IOTA 5 dataset. Reproduced with permission from ⁹. Copyright BMJ Publishing Group.

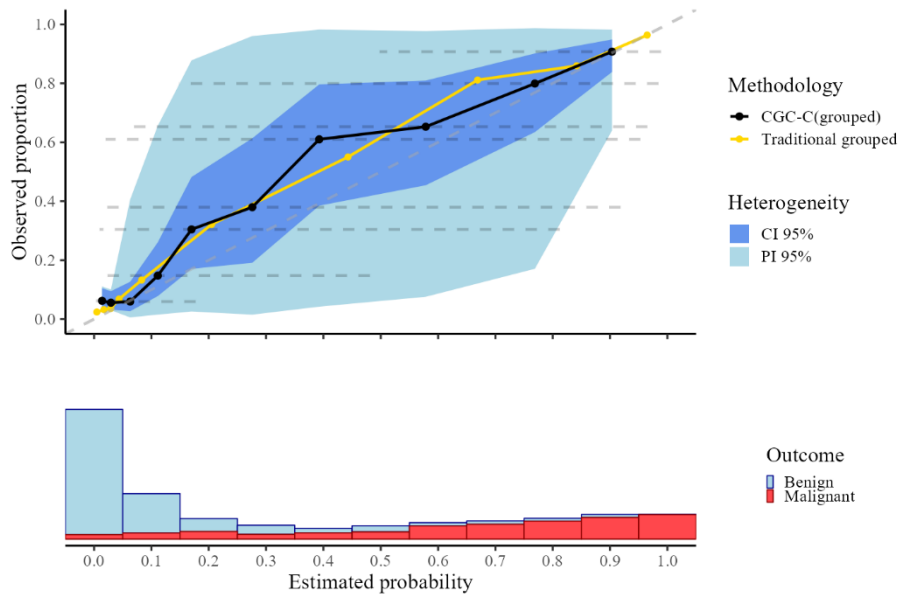


Figure S2. CG-C (grouped) and traditional grouped calibration plot with 10 quantiles and histogram of estimated risks. Dashed line indicates meta-analysis prediction interval across estimated probabilities.

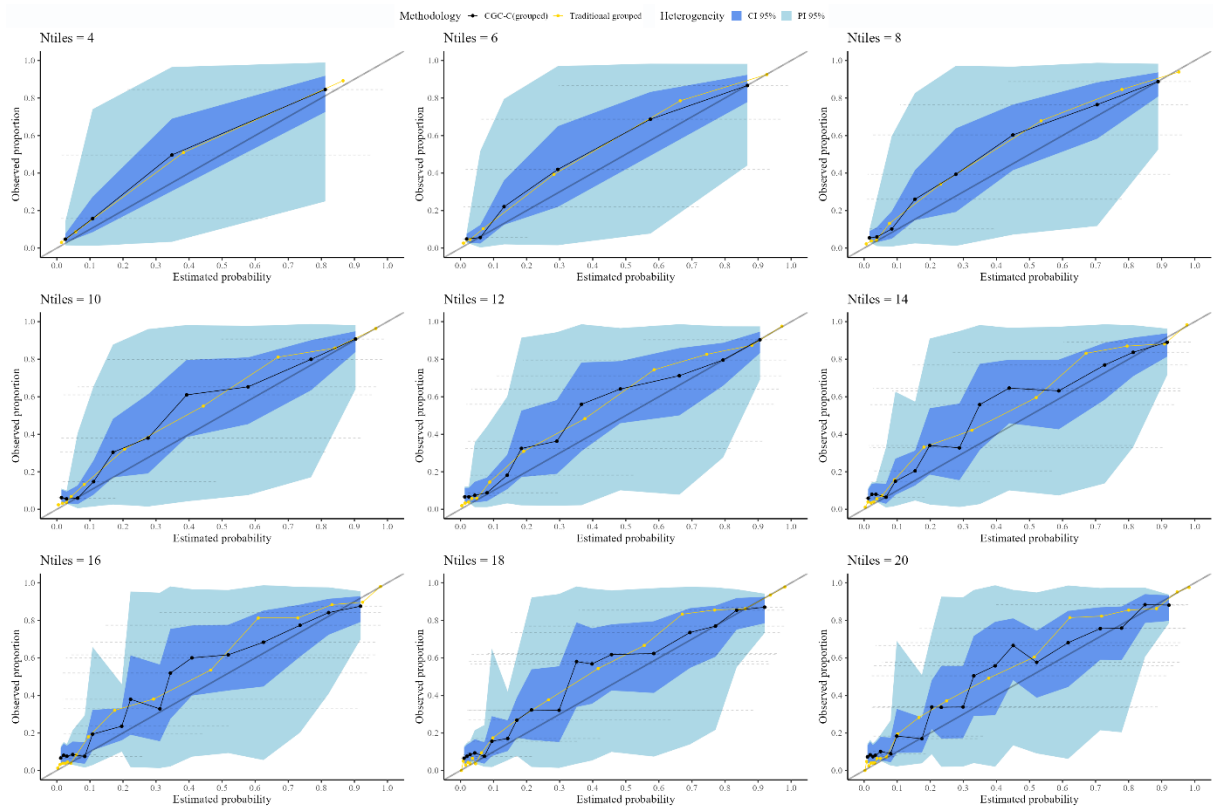


Figure S3. CG-C (grouped) center-specific and traditional grouped calibration plot with varying quantiles from 2 to 20. Dashed line indicates meta-analysis prediction interval across estimated probabilities.

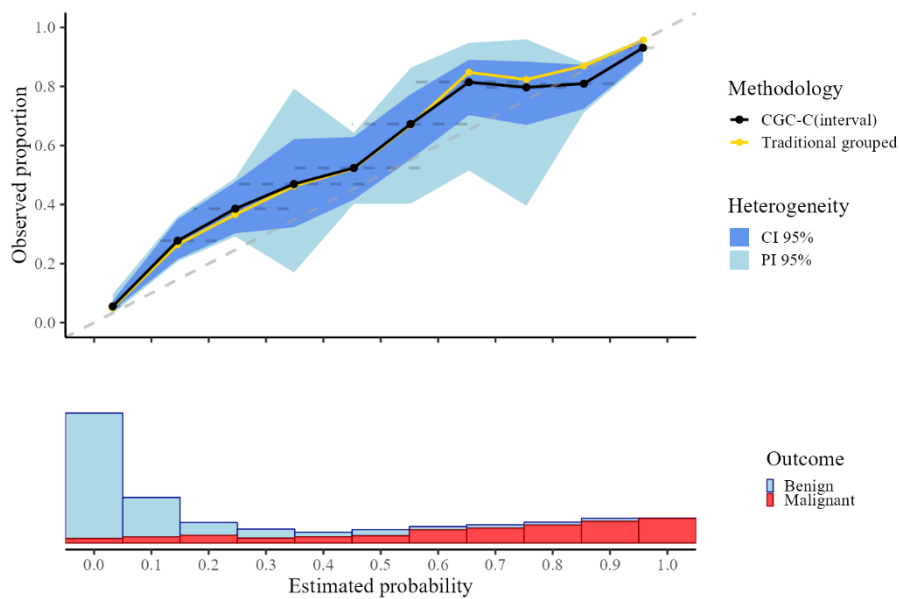


Figure S4. CG-C (interval) and traditional grouped calibration plot with 10 quantiles and histogram of estimated risks. Dashed line indicates meta-analysis prediction interval across estimated probabilities.

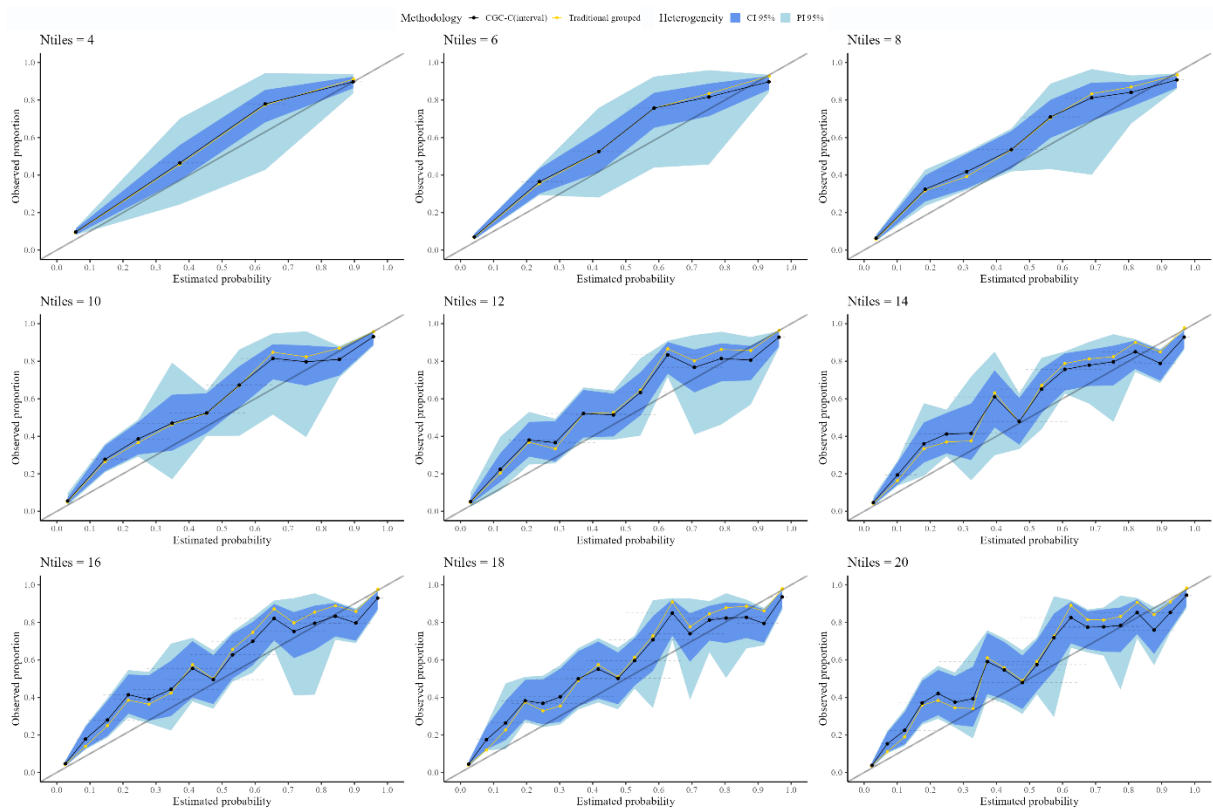


Figure S5. CG-C (interval) center-specific and traditional grouped calibration plot with varying quantiles from 2 to 20.- Dashed line indicates meta-analysis prediction interval across estimated probabilities.

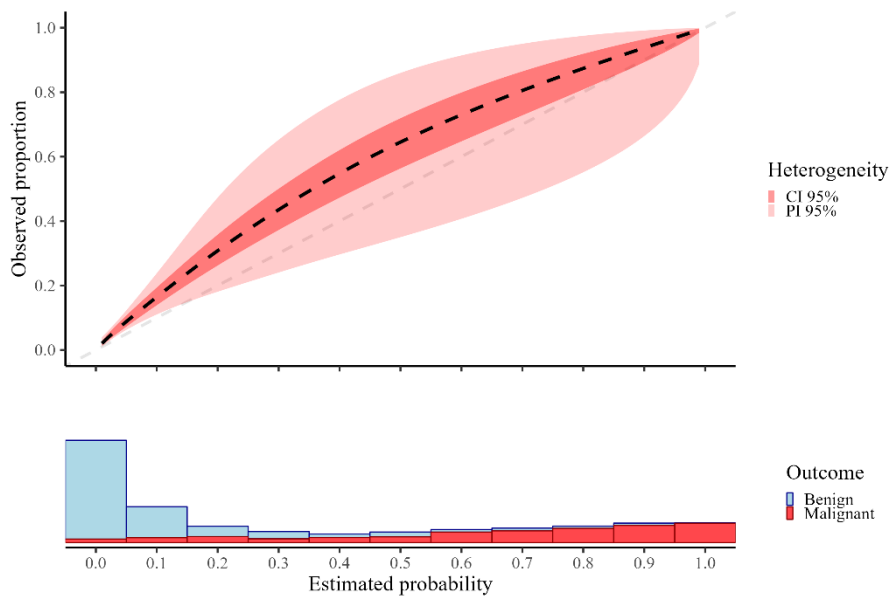


Figure S6. 2MA-C (splines) calibration plot.

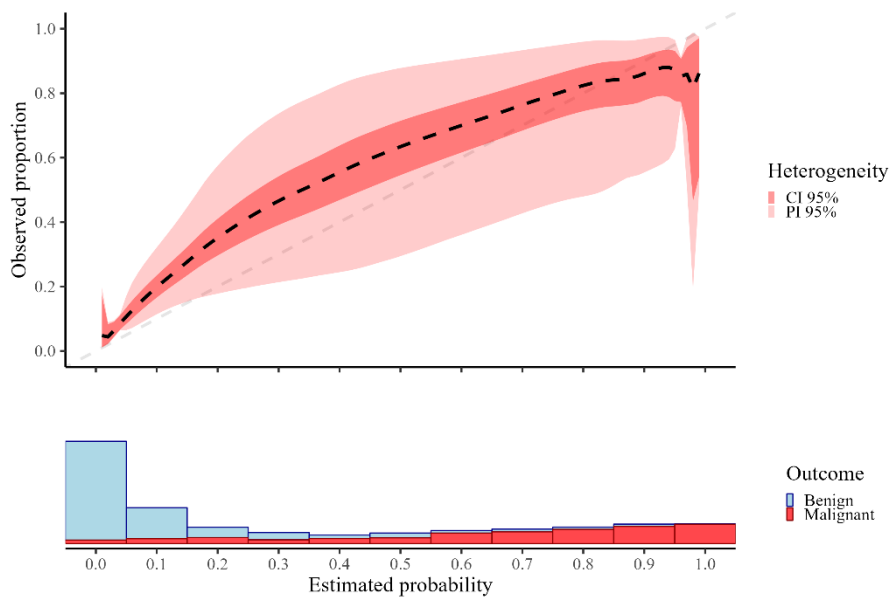


Figure S7. 2MA-C (loess) calibration plot.

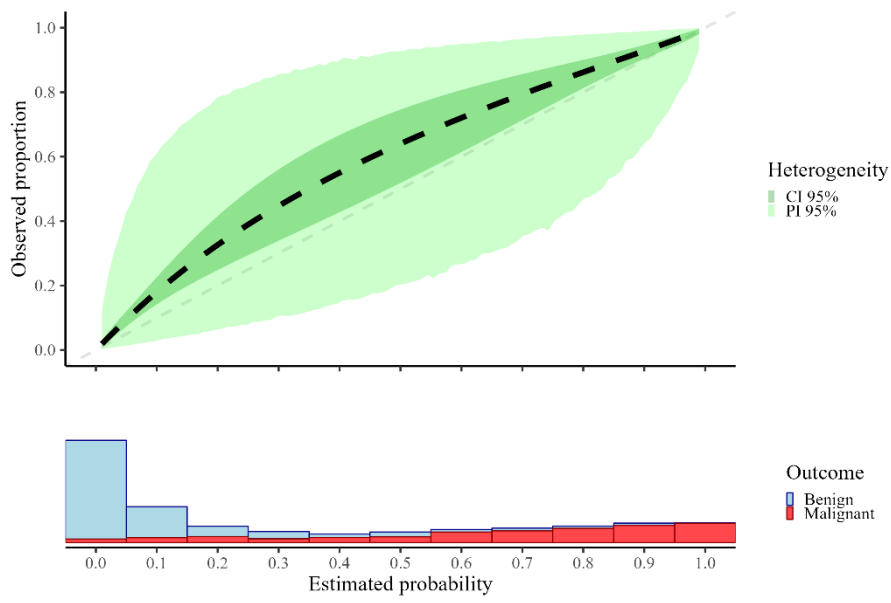


Figure S8. MIX-C calibration curve based on a model with random intercept per center and restricted cubic splines.

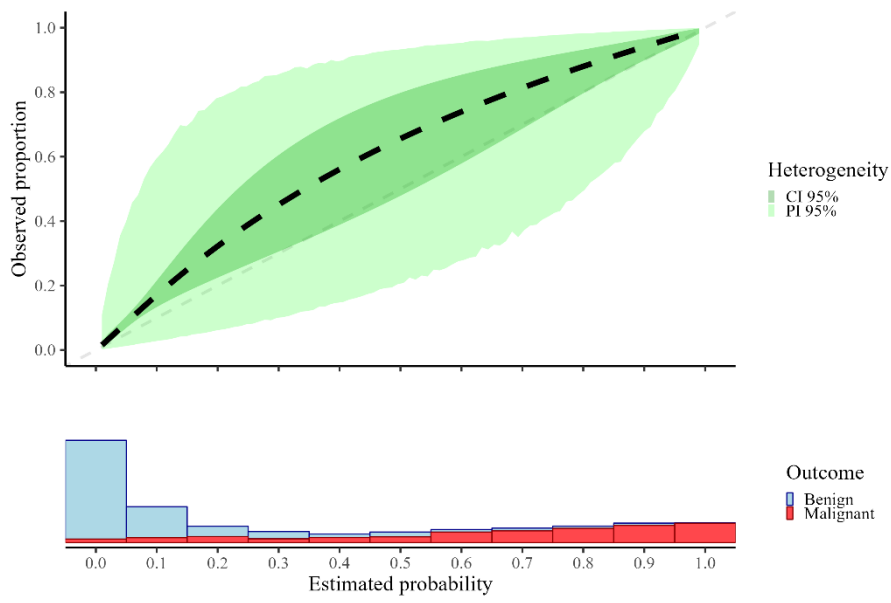


Figure S9. MIX-C calibration curve based on a model with random intercept and slopes per center and restricted cubic splines.

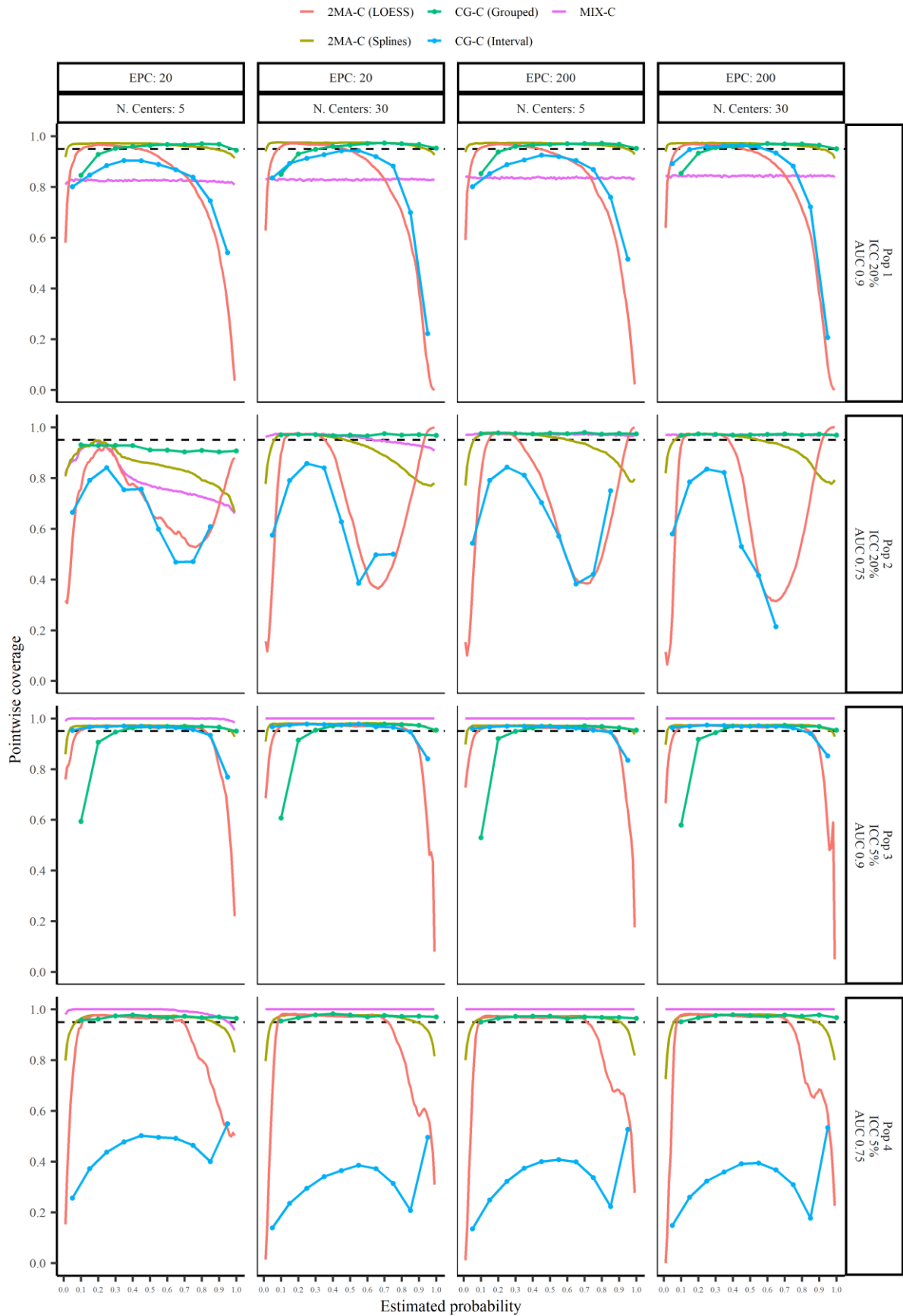


Figure S10. Pointwise heterogeneity average coverage for logistic regression models across the 16 scenarios. Black dotted line indicates nominal coverage (95%).

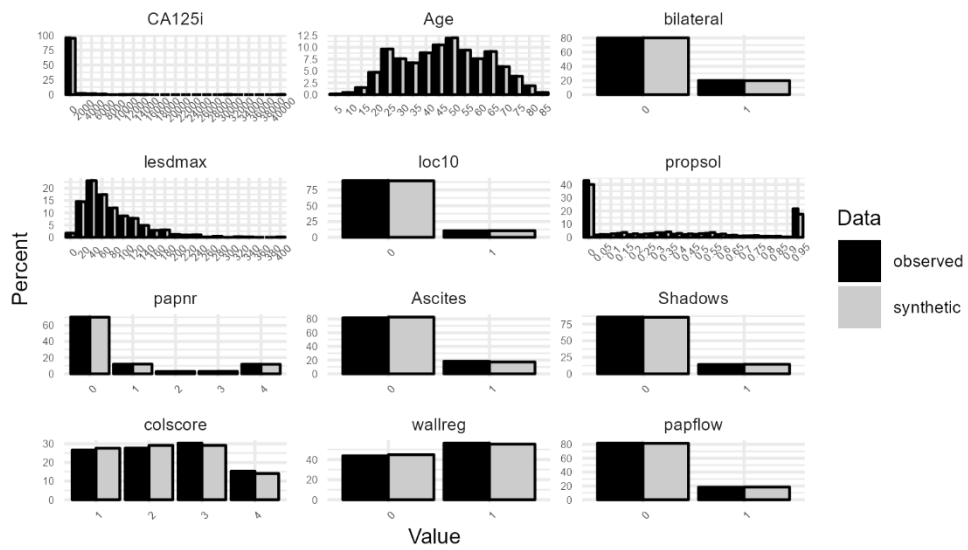


Figure S11. Quality of synthetic data generation for one of the centers (Leuven).

A5. TABLES

Superpopulation	AUC	ICC	ER (range)	Formula
P1	0.9	0.2	0.3 (0.04-0.74)	$\pi(x_{ij}) = -1.6054 - 2.09062x_{ij} + u_j$ $u_j \sim N(0, 1.559)$
P2	0.75	0.2	0.3 (0.05-0.75)	$\pi(x_{ij}) = -1.0122 + 0.4199x_{ij} + u_j$ $u_j \sim N(0, 1.0024)$
P3	0.9	0.05	0.3 (0.14-0.51)	$\pi(x_{ij}) = -1.5943 + 2.3875x_{ij} + u_j$ $u_j \sim N(0, 0.7827)$
P4	0.75	0.05	0.3 (0.14-0.52)	$\pi(x_{ij}) = -1.0244 - 0.9273x_{ij} + u_j$ $u_j \sim N(0, 0.5183)$

Table S1. Superpopulation characteristics